NACA

RESEARCH MEMORANDUM

INVESTIGATION OF COMBUSTION SCREECH AND A METHOD OF ITS CONTROL

By James L. Harp, Jr., Wallace W. Velie, and Lively Bryant

Lewis Flight Propulsion Laboratory
Cleveland, Ohio

NATIONAL ADVISORY COMMITTEE FOR AERONAUTICS

WASHINGTON

March 22, 1954

NATIONAL ADVISORY COMMITTEE FOR AERONAUTICS

RESEARCH MEMORANDUM

INVESTIGATION OF COMBUSTION SCREECH AND A METHOD OF ITS CONTROL

By James L. Harp, Jr., Wallace W. Velie, and Lively Bryant

SUMMARY

An experimental investigation was conducted to determine the cause and to identify the types of pressure oscillations associated with screeching combustion. The tests were conducted in a full-scale turbojet-engine afterburner at sea-level static conditions and in ducted burners of various diameters at various simulated flight conditions.

By means of frequency, phase, and amplitude measurements, it was found that flame-driven transverse resonant oscillations were present during screeching combustion. These oscillations could be completely damped by the installation of a perforated acoustic liner around the inside of the burner wall.

INTRODUCTION

With the development of high-performance afterburners and ram jets, particularly when operating under conditions of high pressure and temperature, a combustion phenomenon generally referred to as "screech" has frequently been encountered. Screech is accompanied by high-frequency pressure oscillations that may be of such magnitude as to cause rapid deterioration of the burner.

Some preliminary experimental investigations at the Lewis laboratory as well as information available from work done elsewhere led to the belief that screech might be, or closely related to, some form of resonant oscillation (standing waves). Flame-driven resonant oscillations in burner tubes (singing flames) have been observed over a period of many years. In 1777, Higgins, while demonstrating that the burning of hydrogen produces water, lowered a vertical glass tube over a hydrogen flame and heard a musical tone from what was probably the first singing flame. There is considerable information available in the literature concerning resonating chambers and flame-driven standing waves (refs. 1 to 4). Data indicating that resonant oscillations are present in rocket motors are presented in references 5 and 6.

With this background of knowledge in mind, an investigation was conducted at the NACA Lewis laboratory to determine if resonant oscillations did exist in screeching afterburner and ram-jet combustors. The frequencies and time histories of the static-pressure variations at various locations in screeching combustors were compared with those to be expected from resonant oscillations. In addition to tests to determine resonance, tests were made to determine if screech was in any way associated with the aerodynamic characteristics of the flow around the flame holder. Based on the information so gained, several configurations designed to eliminate screech were built and tested.

APPARATUS

The investigation of combustion screech was conducted in two separate test facilities, a 26-inch-diameter duct rig and a 32-inch-diameter short afterburner attached to a full-scale turbojet engine; the fuel used in both facilities was MIL-F-5624A grade JP-4.

Ducted burner. - The 26-inch-duct rig (fig. 1(a)) was supplied with air which was combustion preheated to 1250° F; the temperature profile of this air as it entered the diffuser was reasonably uniform. At a station 28 inches upstream of the flame-holder station, fuel was admitted; and at a station 7 inches upstream of the flame-holder station, the initial ignition was accomplished with a torch-type ignitor (as shown in the inset). The burner test section extended approximately 73 inches downstream of the flame-holder station at a constant diameter of 26 inches. Tests were made both with and without the diffuser inner body installed. Tests were also made with ducts of smaller diameters as shown in figures 1(b) and 1(c). The test section of these burners was 36 inches in length in each case, and the duct diameters were 8, 14, and 20 inches. The inlets to the burner sections were faired in with a bellmouth to maintain uniform flow distribution, and the fuel spray bars were redesigned and relocated 9 inches upstream of the flame holder. During one phase of the investigation, a tapered burner (fig. 1(d)) was tested. The burner section extended 45 inches downstream of the flame holder; in this span, it tapered from the original 26-inch duct diameter to an 18.6-inch exit diameter. Runs with the tapered burner were made with the diffuser inner body installed.

The fuel injection system used in the 26-inch duct consisted of 24 spray bars equally spaced circumferentially and located in a plane approximately 28 inches upstream of the flame holder. When the diffuser inner body was installed, the fuel was injected transverse to the air stream through eight 0.020-inch holes (four on each side diametrically opposite). When the inner body was removed, the spray bars were redesigned to supply fuel to the void left by the inner body. In this case, each bar had six 0.020-inch holes pointing upstream. In each configuration the hole spacing was designed on a basis of equal flow area.

Engine afterburner. - A sketch of the full-scale engine and afterburner is shown in figure 2(a), and a detailed sketch of the 32-inch-diameter short afterburner is shown in figure 2(b). Several inner-body configurations were tested, one of which is shown in figure 2(b). The total diffuser length was 18 inches and the total burner length was 36 inches. The two fixed-area exhaust nozzles used had 24.25- and 25.50-inch exit diameters. The fuel-injection system used in the 32-inch afterburner consisted of 16 spray bars, each having 10 spray orifices (five on each side and diametrically opposite) 0.031 inch in diameter and spaced on the center of six equal flow areas (fuel was not sprayed into the outer annulus in order to alleviate excessive heating of the outer shell). The fuel spray was in one plane transverse to the air stream. Spray-bar mounting stations were located 1, $7\frac{1}{2}$, and 13 inches upstream of the flame-holder station.

Configurations tested. - The various flame-holder configurations used for the investigation in the 26-inch-duct rig and the short afterburner are shown in figures 3(a) to 3(h). Configurations 1 and 2 (fig. 3(a)) are double-ring conventional V-gutter flame holders. Configuration 1 was used in the 26-inch-duct rig and configuration 2 was used in the 32-inch-diameter afterburner. Configurations 3 to 9 (fig. 3(b)) are single-ring conventional V-gutter flame holders of various gutter widths and mean ring diameters. Configurations 3 to 7 were used in the 26-inch-duct rig, and configurations 8 and 9 were used in the short afterburner. Splitter modifications of the flame holders are configurations 5a to 5d and 7a (fig. 3(c)). Flame-holder configurations 5a and 5b are models of flame-holder configuration 5 with 6- and 12-inch upstream splitters, respectively. Flame-holder configurations 5c and 7a are modifications of configurations 5 and 7 with circular splitters extending 6 inches downstream of the gutter trailing edge, and flame-holder configuration 5d is a modification of configuration 5 with perpendicular plates extending 6 inches downstream of the trailing edge. An additional form of splitter configuration is flame-holder configuration 10 (fig. 3(d)), which consists of an annular shroud or splitter extending 12 inches downstream from the leading edge of the inner segment of a V-gutter. An additional modification of configuration 5 not shown in a figure consists of a bead made from tubing 1/2 inch in diameter of 0.031 wall thickness which was cut in half and tack welded to each side of the gutter at the leading edge. This flame holder as modified constituted configuration 5e. The diametrical V-gutter flame holders designed for use with the 26-inch-duct rig (configurations 11, 12, and 13) are shown in figure 3(e). The flame holders were mounted at 4 points 90° apart. One-inch tubing was provided within the gutter elements for mounting in the vertical direction, and one-inch tubing enclosed in a faired strut was provided for mounting in the horizontal direction. Configurations 11, 12, and 13 consisted of gutters 5.0, 7.0, and 8.0 inches in width, respectively; configuration 12a is a modification

of configuration 12 with a longitudinal splitter extending 6 inches downstream of the gutter trailing edge and configuration 12b is a modification of configuration 12 with longitudinal and cross splitters extending 6 inches and 9 inches downstream of the gutter trailing edge. The diametrical V-gutter flame holders used in the 20-, 14-, and 8-inch burner test sections are shown in figure 3(f) (configurations 14 to 20). Configurations 14 and 15 were used in the 20-inch duct; configurations 16 to 20 were used in the 14- and 8-inch ducts. A grid-type flame holder, configuration 21, was used in the 26-inch duct. It consisted of 1/2-inch-wide flame-holding elements of the V-gutter and flat-plate type (see fig. 3(g)). The perimeter of the gutter elements was approximately 25.0 inches in diameter. Configurations 22 and 23 (fig. 3(h)), which were tested in the short afterburner, consisted of radial swept V-gutter flame-holding elements attached to a ring which was designed to fit over the downstream end of the inner body.

Additional configurations designed for the purpose of screech elimination were investigated in both the short afterburner and the 26-inch-duct rig. Figure 4(a) is a photograph of longitudinal fins attached to the burner section of the 32-inch-diameter short afterburner. The fins consisted of 25 steel stringers of 2-inch width and 1/8-inch thickness which extended through the burner section as shown in detail in figure 4(b). Another configuration designed for screech attenuation was the perforated acoustic liner. A photograph of the liner installed in the burner section of the short afterburner is shown in figure 5(a) with a flame holder mounted at the flame-holder station. A detailed sketch of the liner installation is shown in figure 5(b). The perforations were 3/16-inch holes on 1/2-inch centers, and the liner was left open at the upstream end for cooling purposes. The downstream end of the liner was closed to direct the cooling air through the perforations. The 26-inch-duct version of the acoustic liner is shown in figures 6(a) and 6(b). The photograph (fig. 6(a)) shows a liner 29 inches long, composed of a 19-inch section with a 10-inch section downstream, as installed in the 26-inch burner. The details of this configuration given in figure 6(b) indicate the method of recessing the burner wall to accommodate the liner in a flush manner with respect to the entrance and exit duct. The 19-inch liner section was filled with an aluminum oxide wool in an attempt to increase the sound absorption qualities.

Instrumentation. - Frequency, phase relations, and relative amplitudes of pressure pulsations during screeching combustion were obtained with microphone-type pressure pickups. The pressure pickup consisted of an electrodynamic microphone capsule enclosed in a brass sheathing as described in reference 7 and shown in figure 7(a). The lead tube attached to the burner and the pickup was extended with a 50-foot coil of tubing to prevent standing waves from occurring in the lead tube

3146

between the wall tap and the pickup. The signal from the pressure pickup was fed into a four-beam oscilloscope through a transformer and a decade amplifier (fig. 7(b)) with provisions made for obtaining permanent tape recordings. The original pressure pickups were uncooled and, therefore, 5-foot lead tubes were used to displace the pickups a reasonable distance from the burner shell. It was soon found, however, that because of unequal heating of the air in the tubes, slight phase shifts were inherent in the system. In order to correct for the phase shifts, the pickups were water cooled, the leads were shortened, and a phase check was made by feeding the same signal from an audio oscillator through the lead tubes to all the pickups. Phase was adjusted by lengthening or shortening the lead tubes as the case dictated.

Reed valves used to read maximum wall pressures are shown in the detailed sketch of figure 8. The reed was mounted on a removable plug and covered a 1/4-inch hole.

Instrumentation used to measure conditions existing in the 26-inch-duct rig and the 32-inch-diameter short afterburner consisted of pressure and temperature rakes to measure burner-inlet total pressure and temperature, and static wall taps at the burner inlet for velocity indications. Air-flow measuring stations were provided for each rig. Afterburner and engine or preheater fuel flows were indicated on fuel rotameters.

PROCEDURE

Various configurations designed to identify the type of oscillation associated with screech were run in the 26-inch-diameter duct. The characteristics of pressure oscillations occurring during screeching combustion were explored through measurements of frequency, phase relations, relative amplitudes, and, in certain cases, stroboscopic observations of the flame front. The screech frequency was determined by matching the frequency of the oscilloscope trace (a 4-beam oscilloscope was used throughout the investigation) fed from the pressure pickups in the burner wall with a signal from an audio oscillator. When the signals were synchronized, the frequency read on the audio oscillator was the screech frequency. Phase relations of the microphones placed at various circumferential or longitudinal positions along the burner wall were determined by comparison of the respective oscilloscope traces. Although quantitative amplitude data for screeching combustion were not obtainable by this method, it was possible to note the change in amplitude of the various signals by initially calibrating the oscilloscope traces for equal gain and then recording the relative change in amplitude for various pressure pickup positions without adjusting the gain settings.

Screech tendency, at given conditions of air flow and pressure, was defined for the purposes of this investigation as the range of fuel-air ratios over which screech was encountered. The greater the range, the greater was the tendency to screech.

In a few specific cases, the frequency of the flame-front oscillation was compared with screech frequency by observing the flame front through a stroboscopic disk.

RESULTS AND DISCUSSION

Oscillation Characteristics

Frequency measurements. - The three types of resonant oscillation believed most likely to occur in a chamber the shape of an afterburner or a ram-jet combustion chamber are longitudinal, radial, and transverse. Figure 9 indicates the particle path for the first two modes of each of these oscillations. The arrowheads in the sketches indicate the nodes, that is, the location of minimum velocity amplitude and maximum pressure amplitude.

The frequency of a longitudinal standing wave in a tube with no over-all gas motion is given by the equation:

$$f = \frac{cn}{2l} \tag{1}$$

where f is the frequency, c is the speed of sound, n is the mode of oscillation, and l is the length of chamber. The frequency of a radial or transverse standing wave in a cylindrical chamber is given by the equation:

$$f = \frac{c\beta}{D} \tag{2}$$

where D is the diameter of the chamber and β is a constant which characterizes the mode of oscillation. The following table gives values of β (from ref. 1) for several modes of oscillation:

Mode	β for transverse oscillation	β for radial oscillation
1	0.5861	1.2197
2	0.9722	2.2331
3	1.3373	3.2383
4	1.6926	4.2411
5	2.0421	

A theoretical plot (on which experimental points are plotted) of frequency against burner diameter for the first five transverse modes of oscillation is presented in figure 10. The plot is based on equation (2), but the values were corrected for stream velocity. For radial and transverse oscillations, it is believed that through-flow must be taken into consideration, because the wave has to buck the stream as it travels across the duct. As the through-flow Mach number increases, the effective velocity of the wave across the duct, and hence the frequency, decreases. It would appear reasonable that the effective velocity of the wave across the duct is equal to the square root of the difference between the speed of sound squared and the stream velocity squared. In computing values for figure 10, a through-flow Mach number of 0.333 was assumed, which was about the average of the experimental data (see table I).

For each mode, a band of frequencies is indicated, the upper and lower limits corresponding to speeds of sound of 2760 feet per second (3500° R) and 2170 feet per second (2100° R), respectively. Because there are large temperature gradients in most combustion chambers, an accurate determination of the effective temperature is not usually possible. However, since frequency is a function of the square root of the temperature, moderate errors in temperature can be tolerated without appreciably affecting the frequency.

Plotted on figure 10 are all the frequencies obtained experimentally in 8-, 14-, 20-, and 26-inch ducts and in the 32-inch-diameter short afterburner, as well as all the frequency data from reference 8. It will be noted that the data definitely fall into bands. With no inner body installed, the frequency data generally fall within the area denoting the first transverse mode; while, with an inner body installed, frequencies corresponding to the higher modes of oscillation are more predominant. In all cases, only frequencies corresponding to the first transverse mode of oscillation were obtained when a diametrical V-gutter flame holder was used with no inner body installed. In some instances with the inner body installed or with a circular-ring flame holder installed with no inner body, the mode of oscillation could be changed by changing the engine operating conditions (for example, changing air flow or fuel-air ratio). It was also observed that for a given

run the frequencies measured at various longitudinal locations were always identical, even though the gas temperature (calculated frequency) at the upstream locations was much lower than the temperature (calculated frequency) at the downstream locations.

Phase and amplitude measurements. - Phase and amplitude measurements are important aids in identifying a resonant oscillation, especially at the higher modes where identification by frequency alone becomes increasingly difficult.

In order to determine if a radial-type oscillation might exist, a pressure pickup was moved from the wall to the center of the 26-inch duct during screeching operation, and the static-pressure variations obtained were compared with a similar reference pickup which remained in a fixed position. The amplitude was maximum at the wall and continually decreased toward the center with no phase shift. With a radial-type oscillation, maximum amplitude would be expected at the center with a 180° phase shift between the wall and the center. Hence, it was concluded that a radial type oscillation did not exist.

Oscilloscope photographs showing the static-pressure variations with time downstream of the diametrical flameholders in the 26-inch duct are presented in figures 11(a) and 11(b). The trace photographs are multiple sweep and the trace width is indicative of the relative gain setting. With both the 5- and the 7-inch-wide gutters, high static-pressure oscillations occurred at opposite ends of the gutter while little oscillation occurred at points 90° to the ends of the gutter. Also, oscillations at opposite ends of the gutter were essentially 180° out of phase. The pressure pickups were connected to the burner wall by 5-foot lead tubes to prevent overheating the pickups (see apparatus), and small phase shifts were believed due to variations in the temperature of the air in the lead tubes. The phase and amplitude relations and frequencies of 560 and 635 cycles per second (figs. 11(a) and 11(b)) are those to be expected with the first transverse mode of oscillation. It would appear that the nodes were located at the gutter ends and that the wave traveled back and forth behind the gutter.

When the gutter width was increased to 8 inches, the wave appeared to oscillate across the gutter instead of parallel to it as was the case with the 5- and 7-inch-wide gutters. Oscilloscope photographs taken with the 8-inch-wide gutter installed are presented in figures 12(a) and 12(b). Little pressure variation occurred at the gutter ends while large oscillations occurred at points 90° to the gutter ends with the latter being 180° out of phase. In this case, water-cooled pressure pickups were used, and the lead tubes were shortened to approximately 8 inches. Before the runs were made, the system was carefully checked to make sure there were no phase shifts inherent in the equipment.

In all runs with the 8-, 14-, and 20-inch ducts, the wave appeared to oscillate across the gutter in the same manner as with the 8-inch-wide gutter in the 26-inch duct. It was observed that, with diametrical flame holders of low blockage, the wave oscillated parallel to the gutter; while, with high blockage, the wave oscillated across the gutter.

With the 5-inch-wide diametrical gutter installed at the trailing end of the innerbody in the 26-inch duct, the observed frequency was 1740 cycles per second. In figure 13 (no oscilloscope photos available), the points marked A were in phase, point B was 180° out of phase, and point C was mostly hash. In this case, the frequency and the phase relations along with the relative amplitudes were those to be expected with the fourth transverse mode of oscillation.

Phase measurements were made with the 2.5-inch circular V-gutter flame holder installed in the 26-inch duct in order to determine if the same phase relations could be obtained with a conventional circular gutter as with a diametrical gutter. Again, it was found that high-amplitude oscillations occurred on opposite sides of the duct, while low-amplitude oscillations occurred at points 90° to the high-amplitude oscillations. It was observed with this flame holder that from run to run the location of the amplitude pattern varied. If screech was stopped (for example, by decreasing fuel-air ratio), the high- and low-pressure regions might rotate and take up new locations when screech was again commenced. However, when once established, the pattern did not appear to rotate as long as the oscillation was maintained.

The 8-inch-wide diametrical V-gutter flame holder was installed in the 26-inch duct, and longitudinal phase measurements were made along the duct with the pickups located on the duct wall in a plane perpendicularly bisecting the flame holder. As mentioned previously, this was the line of maximum amplitude for the 8-inch diametrical gutter. Water-cooled pickups with short lead tubes were used and the equipment was phase checked prior to the run. As shown in figure 14, there was a continual phase change along the portion of the duct where measurements were made. The oscillation in the hot downstream end of the duct consistently leads in phase that in the cooler upstream end.

It will be noted that the distance downstream of the flame holder required for a 180° phase shift was 25 inches, which is essentially the duct diameter. Also, the distance upstream of the flame holder required for a 180° phase shift was 14 inches, which is the amount to be expected for a wave with a frequency of 650 cycles per second and a gas temperature of 1710° R moving against a through-flow stream having a measured velocity of 460 feet per second. Hence, it would appear that there is a traveling wave moving upstream at the same frequency and coupled with the transverse oscillation. A longitudinal standing wave is not indicated because no longitudinal nodes or antinodes were found.

[redacted]

Stroboscopic observations. - Several quartz windows were installed in the side of the 26-inch duct so that the flame front could be observed during screeching combustion. When viewed through a slotted-disk-type stroboscope (8-inch diametrical gutter installed), the flame front was observed to oscillate back and forth over a distance of 4 or 5 inches at 10 inches downstream of the gutter trailing edge. The frequency of the flame-front oscillations was the same as that of the pressure oscillations. No flame-front oscillation could be detected during nonscreeching operation.

Amplitude measurements. - In an attempt to measure the absolute amplitude of the pressure oscillations associated with screech, reed valves with a natural frequency of about 1000 cycles per second were constructed (fig. 8). The operation of each valve was checked in the following manner: The valve was installed in one end of a $1\frac{1}{2}$-inch-diameter tube 38 inches in length; and a 35-watt speaker, used as a source of sound, was installed at the other end of the tube. When resonance (third longitudinal mode) was established in the tube by driving the speaker at about 520 cycles per second, the reed valves indicated a peak pressure of about 25 inches of water above average pressure when properly adjusted. Because of their frequency-response limitation and because of the possible clatter of the reeds against their seal at high amplitudes, the valves were believed to give conservative readings.

Peak static pressures along the 26-inch-diameter burner as measured by the reed valves and average static pressures as measured by conventional static taps are compared in figure 15 for several degrees of screeching combustion. The results, plotted in figure 15, show that the peak static pressure for loud screech was at least 33 percent above the average static pressure and that the region of maximum amplitude was 6 to 10 inches downstream of the flame holder.

Variation of frequency with fuel-air ratio and velocity. - As shown in figure 16, screech frequency increased with fuel-air ratio (temperature) in accordance with theory. The same trend was also observed in the 6-inch duct of reference 8.

It was also found that frequency varied with burner-inlet velocity and pressure as shown in figure 17. For an air-flow of 22.6 pounds per second and a fuel-air ratio of 0.0536, an increase in burner-inlet total pressure from 12.6 to 17.5 inches of mercury absolute and a subsequent decrease in burner-inlet velocity from 1000 to 670 feet per second resulted in an increase in screech frequency from 633 to 718 cycles per second. This increase in frequency was probably caused by a combination of higher combustion efficiency (temperature) and effects of lower through-flow velocities.

Effect of flame-holder aerodynamics. - In reference 9, a water-cooled cylindrical splitter was installed on the single-ring-V-gutter flame holder having a $5\frac{3}{4}$-inch gutter width. This splitter extended downstream from the apex of the gutter in such a manner as to alter the nature of the vortex shedding characteristics of the gutter or possibly to prevent the interaction of the vortices shed by the gutter edges. When this flame holder was installed in a 36-inch-diameter afterburner, screech was not obtained at burner pressures as high as 3850 pounds per square foot absolute, although the same flame holder without the splitter plate screeched at this burner-inlet pressure as well as at pressures as low as 2240 pounds per square foot absolute.

3146

In order to extend the investigation of reference 9, uncooled trailing splitters were installed on the 2.50- and the 4.59-inch-wide single-ring V-gutter flame holders (configurations 5c and 7a). Both splitters extended 6 inches downstream of the gutter edges. Although a slight amount of screech was obtained with these flame holders, the tendency to screech was much less than without the splitters; and only the pressure pickups downstream of the splitters registered any appreciable pressure oscillation. In operation, the trailing edge of the splitters became white hot, but in no instance did any of the splitters melt. Because only the pressure pickups downstream of the splitters indicated any appreciable screech oscillation, it was possible that the splitters could have interfered with the motion of standing waves instead of preventing the interaction of vortices. In order to determine which was the case, a 9-inch-long trailing splitter (configuration 12a) was installed on the 7-inch-wide diametrical gutter. Adding the splitter caused very little change in screech tendency. However, when a cross splitter (configuration 12b) was added to this configuration, the screech tendency was again greatly reduced.

CH-2 back

These and further tests with splitter plates on the 2.5-inch-wide V-gutter single-ring flame holder (configuration 5d) indicated that the splitters stop screech by acting as baffles and interfering with wave motion rather than by altering the aerodynamic characteristics of the flow around the flame holder.

It was observed in the tests of reference 9 that, for a given blocked area, the wider the flame-holder gutters, the greater was the tendency to screech. In order to determine if screech could be completely eliminated by using very narrow gutters, a grid-type flame holder (configuration 21) with gutter widths of 1/2-inch and a total blocked area of 40 percent was constructed. Mild screech at a frequency of 700 cycles per second was obtained when this flame holder was tested in the 26-inch duct.

In order to investigate the possibility that the tendency to screech might be a function of the boundary-layer thickness at the trailing edge of the gutter (larger gutters would naturally build up a thicker boundary layer), a splitter that extended 12 inches upstream of the flame holder was welded to the leading edge of the $2\frac{1}{2}$-inch circular-ring V-gutter (configuration 5b, fig. 3(c)). The intent was to create a thick boundary layer at the flame-holder lips. When tested in the 26-inch duct, this flame-holder configuration considerably increased the tendency to screech as compared with the same flame holder with no leading-edge splitter. A wire tripper was then welded to each side of a 2.5-inch-wide single-ring V-gutter just downstream of the leading edge of the gutter. The purpose of the tripper was to induce a thick boundary layer as in the case of the upstream splitter. When tested in the 26-inch duct, however, this configuration reduced the tendency to screech as compared with the same flame holder without the tripper. No conclusions could be drawn from the results obtained in the gutter-width and boundary-layer tests.

3146

Driving mechanism. - It would appear that the observed resonant oscillations reported herein are basically of the type known as self-excited. The distinction between self-excited and forced vibrations is made clear by the following quotation from reference 10.

"In a self-excited vibration, the alternating force that sustains the motion is created or controlled by the motion itself; when the motion stops, the alternating force disappears.

"In a forced vibration, the sustaining alternating force exits independently of the motion and persists even when the vibratory motion is stopped."

As mentioned previously, flame-driven resonant oscillations in burner tubes have been observed for many years. Rayleigh (ref. 2), in advancing his explanation of singing flames, said that the oscillation is driven by the periodic addition of heat to the air at locations where the pressure varies and at the moment of greatest condensation. The mechanism for self-excitation in combustion systems is believed adequately explained by the following quotation from reference 5:

"A mechanism for self-exicitation using the energy of the combustion process is suggested by consideration of the following facts: (1) Acoustical oscillations are associated with periodic variations in pressure and temperature in time and in space. These variations are in the same direction at any point at any instant; (2) Rates of combustion reactions, and chemical reactions in general, increase with temperature. Furthermore, even in the absence of temperature variations, the effect of a pressure increase alone is to increase the mass rate

of reaction in a flame. Data for various gases are quoted by Jost [ref. 11], which show that, although the linear flame speed may decrease with pressure, in no case does it decrease as rapidly as 1/p [p is the chamber pressure], so that the "mass flame speed" increases, and therewith the rate of liberation of energy; (3) Acoustical oscillations can be sustained and amplified by the periodic addition of heat (or compression) in phase with the pressure variation (Rayleigh's principle, . . .).

"Combination of the above principles leads to the following as a possible self-excitation mechanism in combustion systems: a small-amplitude acoustical oscillation, initiated by some minor disturbance (perhaps a flow oscillation), causes periodic fluctuations in pressure and temperature within a zone of combustion reaction (gas phase); these fluctuations induce sympathetic fluctuations in the rate of reaction and hence of energy liberation in the form of heat and potential expansion work; if there is no appreciable time lag in the process, extra energy is liberated in phase with the pressure increase (and less energy is liberated during the rarefaction phase); the induced periodicity in the energy supply amplifies the oscillation, in accordance with the . . . Rayleigh principle."

The foregoing quotation from reference 5 refers particularly to the driving mechanism of rocket oscillations, but is believed to apply equally well to oscillations in afterburners and ram jets.

Methods of Screech Elimination

Longitudinal fins. - In an attempt to eliminate screech in the 32-inch short afterburner, strips of metal were welded to the inside of the burner at 4-inch intervals around the circumference (fig. 4) to interfere with the wave motion. These fins were 1/8-inch thick, projected 2 inches into the stream, and extended from 6 inches upstream of the flame holder to 6 inches upstream of the exhaust nozzle. It was felt that the strips would not withstand the extreme heat if projected more than 2 inches into the stream. The screech tendency was somewhat reduced, allowing an over-all fuel-air ratio increase from 0.043 to 0.054 before screech was encountered. The most significant information gained, however, was that the screech frequency increased from 1560 to 1760 cycles per second. This increase in frequency is the same as that which would be expected if the duct diameter were decreased 4 inches (see fig. 10); therefore, the wave was probably oscillating just inside the fins.

Tapered burner. - It was believed that a tapered burner might eliminate screech, since at all points along the burner a different calculated frequency exists. Consequently, a burner 45 inches long

was constructed (fig. 1(d)); the diameter of this burner decreased from 26.0 inches at the inlet to 18.6 inches at the exit. This was the maximum taper believed practical. The burner was tested in the 26-inch-duct rig with the inner body installed, and no difference in screech tendency was observed over that of a straight walled burner. These results are consistent with the earlier findings that a straight walled burner will screech even though the calculated frequency at the inlet is different from that at the exit because of the temperature rise through the burner.

Perforated acoustic liner. - Since devices designed to interfere with wave motion did not prove entirely successful, it was believed that an acoustic liner designed to absorb the oscillation might prove more successful. A liner (figs. 5(a) and 5(b)) was designed from information given in reference 12; data given therein indicate that this liner should absorb about 85 percent of the incident sound at the screech frequencies encountered. The liner tested in the short afterburner was 24 inches in length and ran from 6 inches ahead of the flame holder to the beginning of the tapered exhaust nozzle. Screech was completely eliminated regardless of flame-holder size, fuel distribution, or fuel-air ratio. This result was felt to be particularly significant, since this afterburner possessed very strong screech tendencies without the liner.

Additional tests were conducted with an acoustic liner (figs. 6(a) and 6(b)) and the 4.59-inch-wide V-gutter single-ring flame holder (configuration 7) installed in the 26-inch duct. The burner screeched at all conditions investigated when no liner was used (fig. 18). At a burner-inlet pressure of 1400 pounds per square foot, screech was eliminated when the 19-inch-long acoustic liner was used; only relatively light screech was obtained at burner-inlet pressures of 1750 pounds per square foot at fuel-air ratios from 0.05 to 0.08. The addition of another 10 inches of liner length (29-inch total length) completely eliminated screech over the entire fuel-air ratio range for all pressures investigated (up to 2200 lb/sq ft). The use of the perforated acoustic liner was by far the most successful method of eliminating screech.

The acoustic liner used in the short afterburner also served as a cooling liner with the relatively cool turbine-outlet gases flowing between the liner and the afterburner shell. It was very effective in eliminating several severe hot spots on the burner shell which had continually been encountered. The liner used in the short afterburner was essentially free of buckling and warping, whereas the uncooled liner used in the 26-inch duct was badly buckled after a relatively few hours of operation.

The 19-inch section had aluminum oxide wool located between the liner and burner shell, whereas the 10-inch section did not. It was

believed that the wool might increase the sound absorption qualities of the liner. However, no difference in absorption properties was observed between the two liners. The wool tended to aggravate the liner cooling problem, the buckling of the 19-inch liner section being much worse than the 10-inch section.

CONCLUDING REMARKS

The results of this investigation confirm that standing waves are present within the combustion chamber during screeching combustion. The frequency, phase, and amplitude relations observed were those to be expected from the first five transverse modes of oscillation. There was a definite tendency for the higher modes of oscillation to occur with an inner body installed in the burner and for the lower modes to occur with no inner body. Maximum peak static pressures occurred 6 to 10 inches downstream of the flame holder and were about 33 percent greater than the average static pressure.

On the basis of the configurations investigated, the perforated acoustic liner appeared to be a reliable method for the elimination of screech. When air was allowed to flow into the upstream end of the perforated liner (as in the case with the short afterburner), the acoustic liner also served as a cooling liner, which considerably reduced the afterburner shell temperatures.

Lewis Flight Propulsion Laboratory
National Advisory Committee for Aeronautics
Cleveland, Ohio, January 12, 1954

REFERENCES

1. Morse, Philip M.: Vibration and Sound. Second ed., McGraw-Hill Book Co., Inc., 1948.

2. Rayleigh: Theory of Sound. Vol. II. Dover Pub., 1945.

3. Putnam, Abbott A., and Dennis, William R.: A Study of Burner Oscillations of the Organ-Pipe Type. Presented at A.S.M.E. meeting (Cincinnati), June 15-19, 1952.

4. Blackshear, Perry L.: Driving Standing Waves by Heat Addition. NACA TN 2772, 1952.

5. Smith, R. P., and Sprenger, D. F.: Combustion Instability in Solid-Propellant Rockets. Fourth Symposium (International) on Combustion, The Williams & Wilkins Co., 1953, pp. 893-906.

6. Tischler, Adelbert O., Massa, Rudolph V., and Mantler, Raymond L.: An Investigation of High-Frequency Combustion Oscillations in Liquid-Propellant Rocket Engines. NACA RM E53B27, 1953.

7. Beranek, Leo L.: Acoustic Measurements. John Wiley & Sons, Inc. 1949.

8. Bragdon, Thomas A., Lewis, George D., and King, Charles H.: Interim Report on Experimental Investigation of High Frequency Oscillations in Ramjet Combustion Chambers. M.I.T. Meteor Rep. UAC-53, Res. Dept., United Aircraft Corp., Oct. 1951. (BuOrd Contract NOrd 9845.)

9. Usow, Karl H., Meyer, Carl L., and Schulze, Frederick W.: Experimental Investigation of Screeching Combustion in Full-Scale Afterburner. NACA RM E53I01, 1953.

10. Den Hartog, J. P.: Mechanical Vibrations. Third ed., McGraw-Hill Book Co., Inc. 1947, ch. VII.

11. Jost, Wilhelm: Explosion and Combustion Processes in Gases. McGraw-Hill Book Co., Inc., 1946, p. 90.

12. Marks, Lionel S.: Mechanical Engineer's Handbook. Fifth ed., McGraw-Hill Book Co., Inc., 1951.

TABLE I. - EXPERIMENTAL DATA

Run	Burner diameter, in.	Flame-holder configuration		Flame-holder blockage, percent[a]	Air flow, lb/sec	Burner-inlet total pressure, in. Hg abs	Burner-inlet Mach number	Overall fuel-air ratio	Inner body	Screech frequency, cps
		Figure	Configuration							
1	26.0	3(b)	6	29.4	22.6	16.6	0.366	0.0544	Yes	730
2						17.1	.351	.0544		730
3						15.7	.397	.0544		730
4						13.5	.473	.0544		730
5						13.5	.460	.0362		610
6	26.0	3(b)	6	29.4	22.6	13.5	0.462	0.0401	Yes	620
7						13.8	.453	.0444		655
8						13.7	.463	.0535		658
9						15.9	.376	.0418		675
10						16.0	.375	.0442		688
11	26.0	3(b)	6	29.4	22.6	16.0	0.376	0.0490	Yes	698
12						16.2	.380	.0536		717
13						16.2	.380	.0592		720
14						12.6	.514	.0535		633
15						13.9	.455	.0537		660
16	26.0	3(b)	6	29.4	22.6	14.9	0.414	0.0537	Yes	680
17						15.7	.397	.0536		710
18						16.7	.360	.0536		710
19						17.5	.340	.0535		718
20					20.3	24.2	.213	.0432		2015
21	26.0	3(b)	6	29.4	20.3	17.0	0.336	0.0530	Yes	1960
22					20.3	16.6	.360	.0659		1610
23					15.6	13.8	.324	.0568		1980
24						13.4	.337	.0614		1980
25						13.2	.338	.0658		1980
26	26.0	3(b)	6	29.4	15.6	19.0	0.246	0.0478	Yes	1460
27					15.6	23.0	.182	.0433		1460
28					10.6	16.4	.182	.0575		2050
29						12.2	.252	.0624		2050
30						11.1	.277	.0671		2010
31	26.0	3(b)	6	29.4	10.6	21.6	0.143	0.0522	Yes	2060
32			3	14.8	24.5	21.4	.306	.0655		1480
33					24.5	----	-----	.0651		1360
34					20.6	23.8	.229	.0492		1570
35					20.6	17.6	.313	.0663		1540
36	26.0	3(b)	3	14.8	20.6	16.7	0.335	0.0712	Yes	1550
37					20.6	17.5	.324	.0755		1550
38					15.2	18.4	.208	.0534		1590
39						14.7	.270	.0581		1590
40						11.9	.349	.0628		1590
41	26.0	3(b)	3	14.8	15.2	11.3	0.364	0.0673	Yes	1590
42					15.2	11.9	.353	.0768		1590
43					9.9	12.4	.210	.0646		1590
44			4	16.6	24.3	19.1	.306	.0531		630
45			4	16.6	19.5	18.4	.242	.0512		1710
46	26.0	3(b)	4	16.6	19.5	19.4	0.228	0.0567	Yes	1610
47					15.6	15.7	.228	.0556		1570
48					15.6	15.9	.225	.0619		1600
49			5	24.0	19.7	18.6	.250	.0616		1600
50			5	24.0	19.7	15.6	.302	.0613		1540
51	26.0	3(b)	5	24.0	19.7	13.9	0.346	0.0740	Yes	1460
52					19.7	18.2	.258	.0737		1560
53					10.0	13.5	.185	.0765		1660
54		3(e)	12	31.4	20.3	25.0	.156	.0591	No	635
55		3(e)	13	35.3	24.2	15.7	.234	.0622	No	650
56	26.0	3(e)	12a	31.4	20.9	13.2	0.327	0.0640	No	625
57		3(c)	5a	23.8	17.7	14.0	.255	.0575		640
58		3(e)	12b	31.4	20.7	12.8	.334	.0717		650
59		3(c)	5d	23.8	20.6	14.8	.277	.0601		1100
60		3(a)	1	39.5	20.6	15.3	.265	.0607		655 and 1110

[a]Based on burner cross-sectional area.

[redacted]

TABLE I. - Concluded. EXPERIMENTAL DATA

Run	Burner diameter, in.	Flame-holder configuration		Flame-holder blockage, percent[b]	Air flow, lb/sec	Burner-inlet total pressure, in. Hg abs	Burner-inlet Mach number	Overall fuel-air ratio	Inner body	Screech frequency, cps
		Figure	Configuration							
61	26.0	3(d)	10	26.5	20.5	18.1	0.222	0.0577	No	700
62	↓	3(g)	21	40.0	20.4	14.9	.280	.0598		700
63		3(c)	7a	35.7	19.6	13.0	.307	.0624		620
64		3(f)	7	35.7	21.5	12.4	.368	.0579		590
65	8.0	3(f)	18	33.9	6.0	33.8	.402	.0919		1760
66	8.0	3(f)	18	35.9	6.0	37.2	0.358	0.0919	No	1830
67	↓		19	24.7	8.1	40.8	.434	.0588	↓	1680
68			↓	54.1	4.2	37.4	.258	.0667		2170
69				54.1	4.2	38.5	.224	.0811		2130
70	26.0	3(a)	1	39.5	14.8	11.0	.298	.0636	Yes	1070
71	26.0	3(a)	1	39.5	14.8	11.4	0.290	0.0891	Yes	1090
72					↓	10.1	.326	.0695		1020
73						12.1	.282	.0748		1125
74						10.2	.320	.0750		630
75					19.7	14.3	.303	.0567		1070
76	26.0	3(a)	1	39.5	19.7	12.8	0.342	0.0568	Yes	975
77		↓	↓	↓	↓	16.1	.282	.0678		1125
78						16.4	.265	.0740		1140
79		3(e)	11	23.6	19.9	18.4	.234	.0608		1670
80		3(e)	11	23.6	19.9	19.6	.217	.0683		1710
81	26.0	3(e)	11	23.6	19.9	19.2	0.211	0.0611	Yes	1740
82					↓	20.5	.210	.0611		1740
83						22.4	.193	.0615		1680
84					15.3	15.3	.222	.0836		1680
85					15.3	15.5	.218	.0851		1680
86	26.0	3(e)	11	23.6	15.3	15.5	0.218	0.0837	Yes	1680
87		3(c)	7a	35.7	25.0	17.5	.287	.0489	No	650
88		3(b)	5	23.8	20.9	14.5	.227	.0604	↓	640
89		3(c)	5b	↓	15.4	16.7	.172	.0378		630
90		3(c)	5b		21.5	22.1	.185	.0571		650
91	26.0	3(e)	11	23.6	29.2	14.3	0.429	0.0597	No	550
92	↓	----	5e	23.8	30.0	13.0	.314	.0619		650
93		3(c)	5c	23.8	30.5	16.7	.368	.0347		960
94	14.0	3(f)	17	46.4	12.2	33.1	.244	.0608		1290
95	14.0	3(f)	17	46.4	8.4	24.0	.234	.0626		1250
96	14.0	3(f)	17	46.4	8.4	31.4	0.177	0.0610	No	1340
97	↓		↓	↓	12.3	32.1	.324	.0753		1240
98					14.3	35.8	.250	.0655		1220
99					14.3	36.6	.224	.0676		1200
100			16	34.1	16.9	32.9	.364	.0723		1080
101	14.0	3(f)	16	34.1	18.6	37.4	0.349	0.0710	No	1090
102	20.0		14	45.4	20.8	28.7	.235	.0666		800
103			↓	↓	20.8	27.5	.246	.0676		760
104					12.1	20.4	.194	.0718		780
105	↓		15	54.5	21.0	31.8	.214	.0638		900
106	20.0	3(f)	15	54.5	21.0	34.0	0.200	0.0631	No	930
107	Tapered	3(b)	7	35.7	19.1	14.2	.278	.0832	Yes	1820
108	↓	↓	↓	↓	↓	14.6	.272	.0806	↓	1845
109						14.9	.260	.0790		1885
110						15.2	.253	.0754		1925
111	Tapered	3(b)	7	35.7	19.1	15.3	0.251	0.0730	Yes	1940
112	↓	↓	↓	↓	↓	15.4	.251	.0709		1955
113						15.8	.244	.0709		1950
114	32	3(h)	22	31.5	90-100	51.0	.25	.037		1580
115	32	3(b)	9	20.8	90-100	51.0	.25	.044		780
116	32	3(b)	9	20.8	90-100	51.0	0.25	0.045	Yes	1600
117		No flame holder						.039		1360
118		3(h)	22	31.5				.038		1360
119		3(b)	9	20.8				.040		1560
120		3(b)	9	20.8				.040		1520
121	32	3(h)	22	31.5	90-100	51.0	0.25	0.048	Yes	1330
122		3(h)	22	31.5				.043		1350
123		3(a)	2	28.4				-----		1300
124		3(h)	23	25.8				.036		1160
125		3(a)	2	28.4				.043		1560
126	32	3(a)	2	28.4	90-100	51.0	0.25	0.054	Yes	1760
127		3(a)	2	28.4				.053		1320
128		3(b)	8	36.8				.053		1240
129		3(a)	2	28.4				.037		1470

[b]For runs 114 through 129, the blunt-end area of the inner body was considered part of flame-holder blockage.

[redacted]

3146

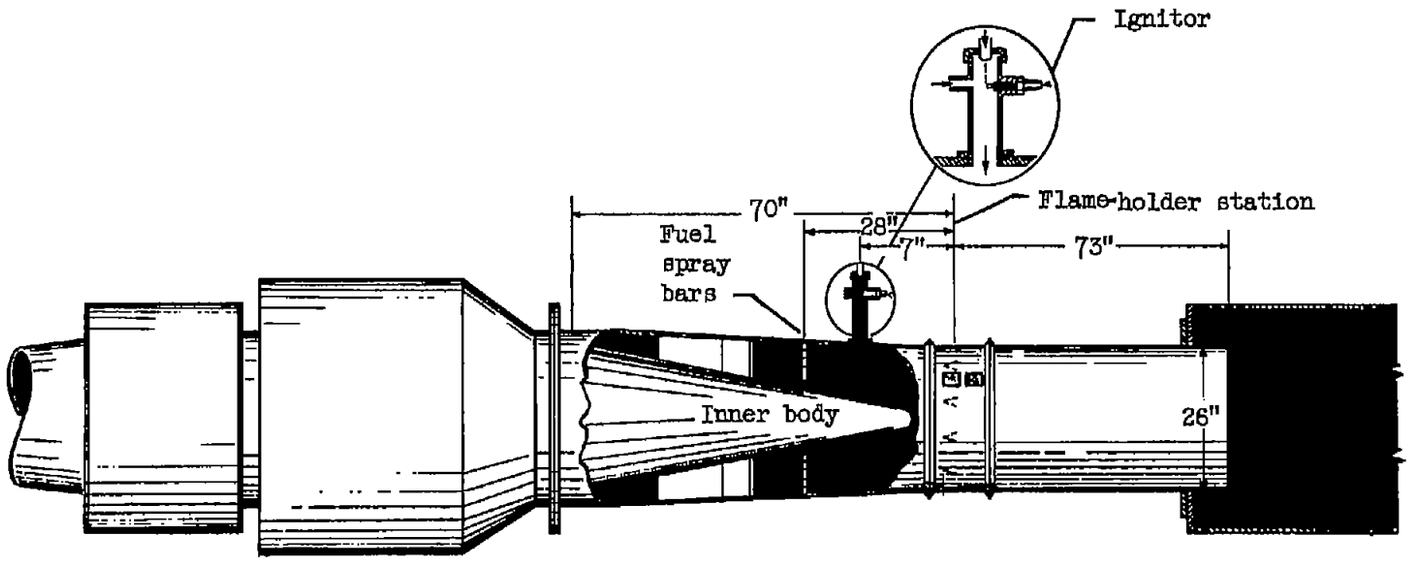

(a) 26-Inch-duct rig (tests were made with and without inner body installed).

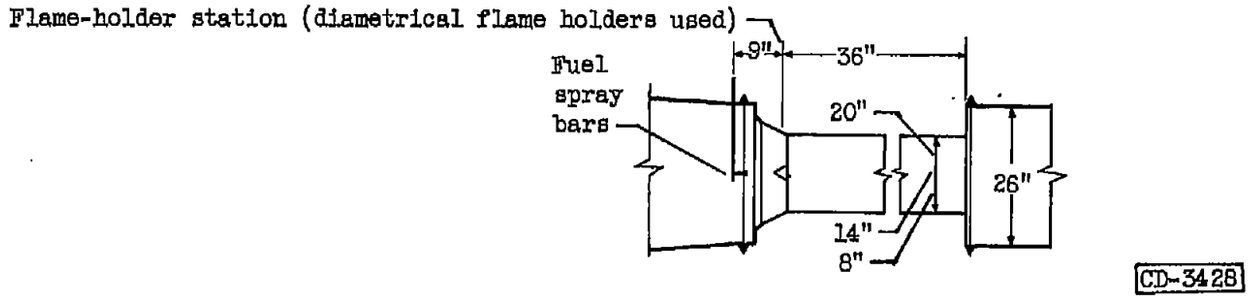

(b) 20-, 14-, and 8-Inch ducts used.

Figure 1. - Various ducts used in investigation.

(c) 8-Inch-duct section run in 26-inch rig.

Figure 1. - Continued. Various ducts used in investigation.

(d) Sketch of tapered burner section used in 26-inch-diameter duct rig.

Figure 1. - Concluded. Various ducts used in investigation.

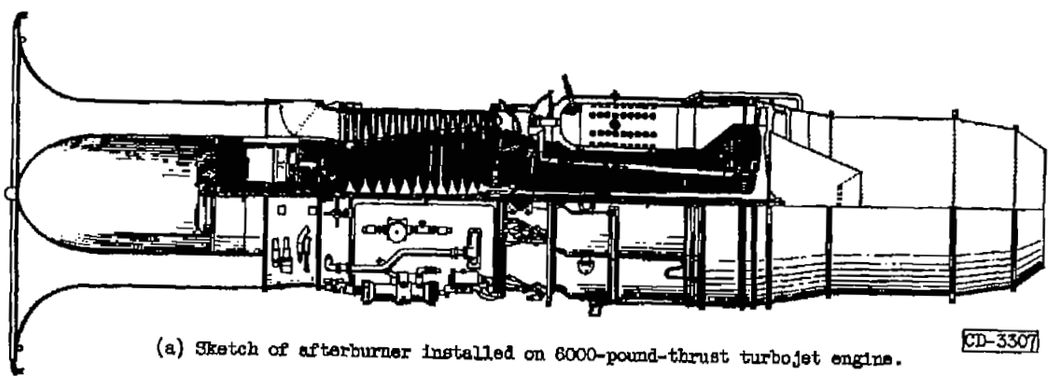

(a) Sketch of afterburner installed on 6000-pound-thrust turbojet engine. CD-3307

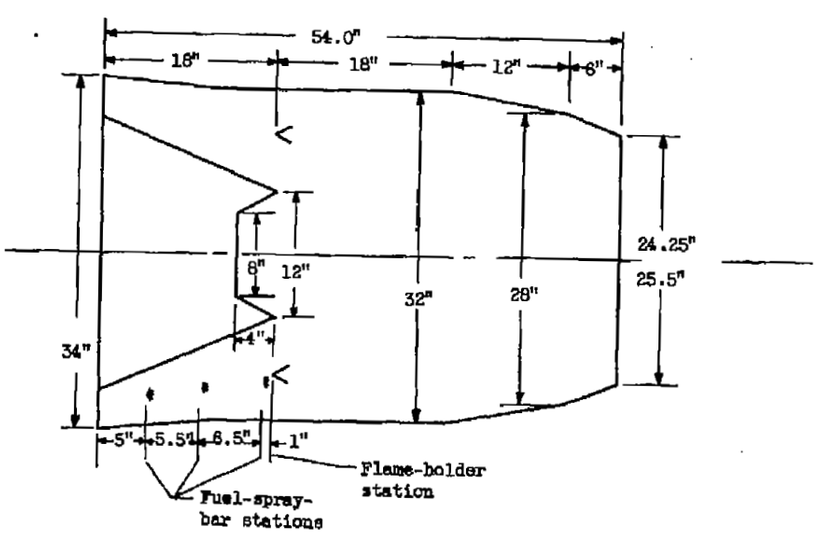

(b) Sketch with dimensions of afterburner.

Figure 2. - Sketch and schematic diagram of 32-inch-diameter afterburner.

Configurations 1 and 2

Configuration	A	B	C	D	E
1	22.65	16.50	1.50	34°	0
2	25.50	19.50	.75	35°	.62

(a) Double-ring conventional V-gutter flame holders.

Figure 3. - Flame holders used for investigations in 26-inch duct and 32-inch afterburner. (Linear dimensions in inches).

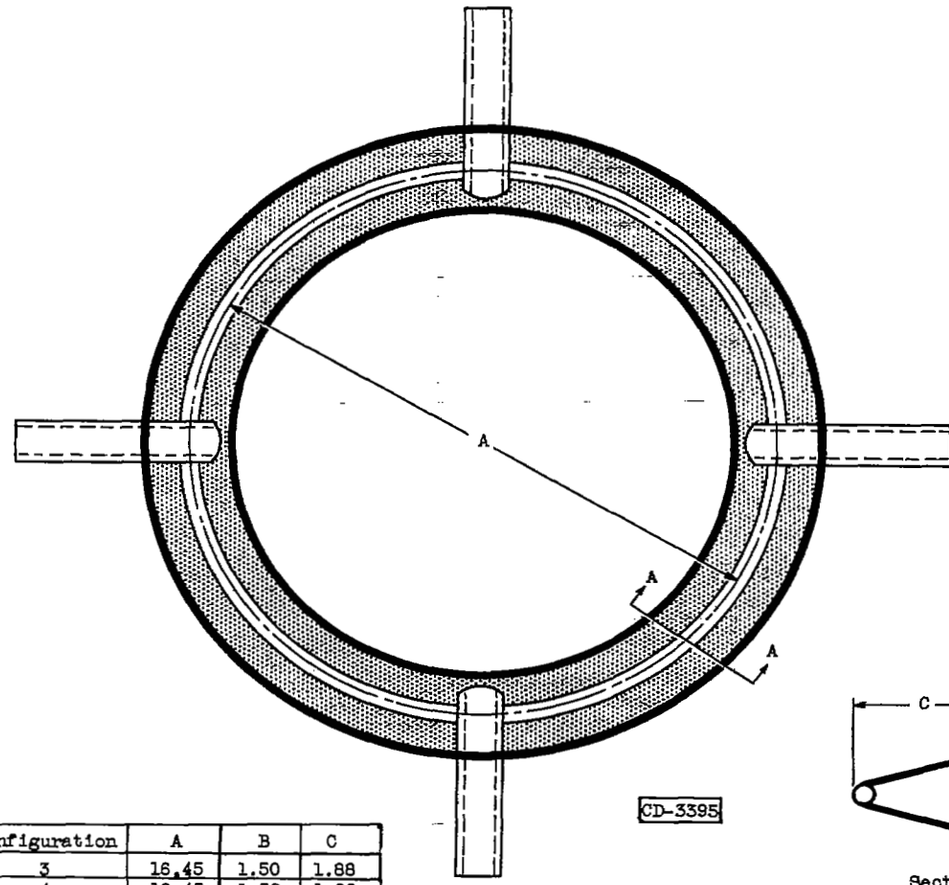

Section A-A

Configuration	A	B	C
3	16.45	1.50	1.88
4	19.45	1.50	1.88
5	15.92	2.50	3.56
6	19.45	2.50	3.56
7	13.00	4.59	7.00
8	23.25	2.50	3.65
9	23.25	0.75	1.12

Configurations 3 to 9

(b) Single-ring conventional V-gutter flame holders.

Figure 3. - Continued. Flame holders used for investigations in 26-inch duct and 32-inch afterburner. (Linear dimensions in inches).

[redacted]

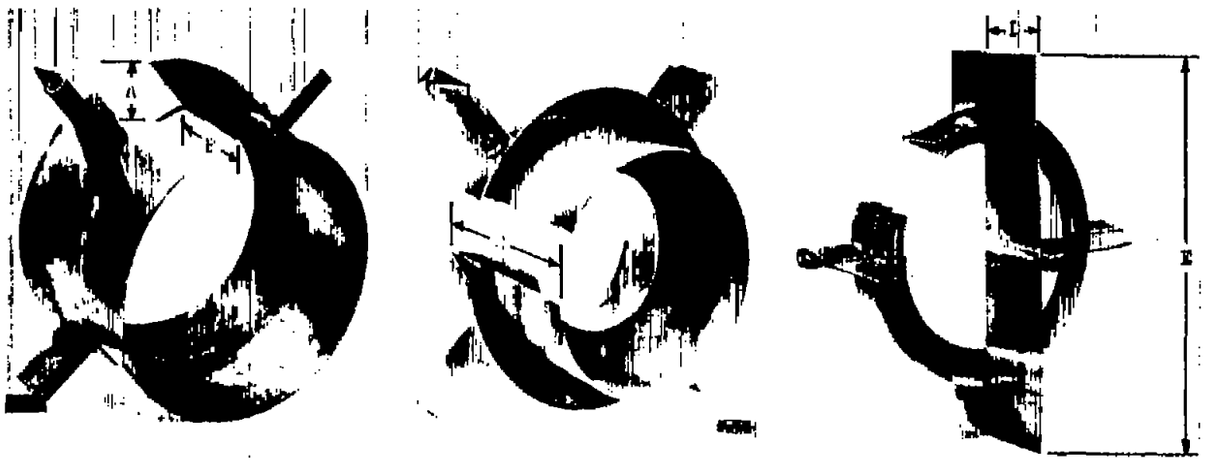

Configurations 5a and 5b | Configurations 5c and 7a | Configuration 5d

CD-3398

Configuration	A	B	C	D	E
5a	2.50	6.00			
5b	2.50	12.00			
5c	2.50		9.56		
7a	4.59		13.00		
5d	2.50			6.00	25.25

(c) Splitter modifications of conventional V-gutter flame holders used.

Figure 3. - Continued. Flame holders used for investigations in 26-inch duct and 32-inch afterburner. (Linear dimensions in inches).

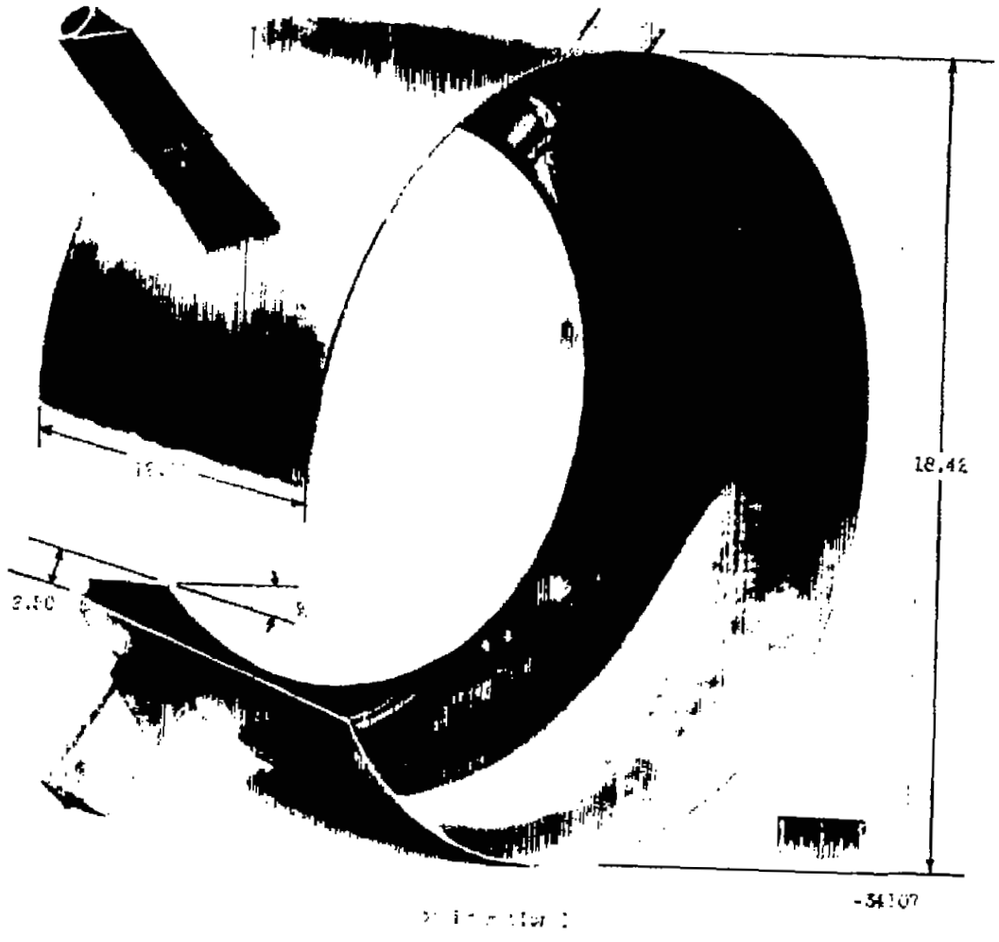

(d) Half V-gutter flame holder with splitter.

Figure 3. - Continued. Flame holders used for investigations in 26-inch duct and 32-inch afterburner. (Linear dimensions in inches).

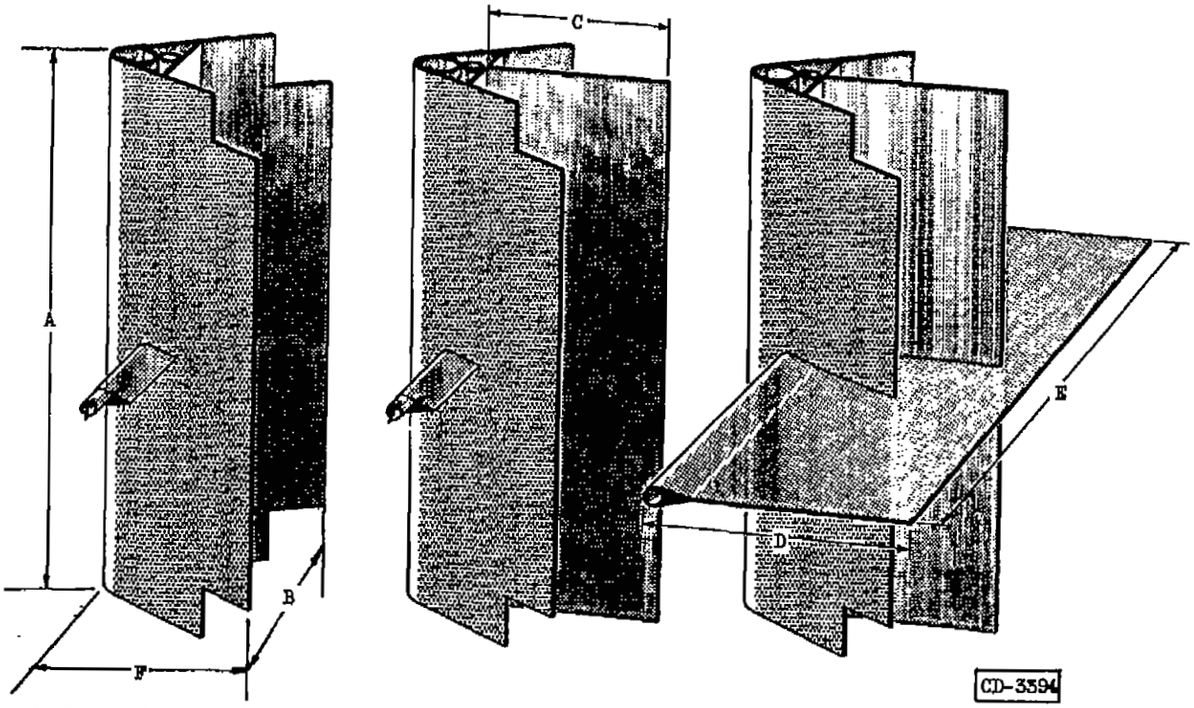

Configurations 11, 12, and 13 Configuration 12a Configuration 12b

Configuration	A	B	C	D	E	F
11	24.75	5.0				5.8
12	24.75	7.0				9.0
13	24.75	8.0				9.0
12a	24.75	7.0	12.00			9.0
12b	24.75	7.0	12.00	16.00	25.25	9.0

(e) Diametrical flame-holder configurations and modifications used in 26-inch duct.

Figure 3. - Continued. Flame holders used for investigations in 26-inch duct and 32-inch afterburner. (Linear dimensions in inches).

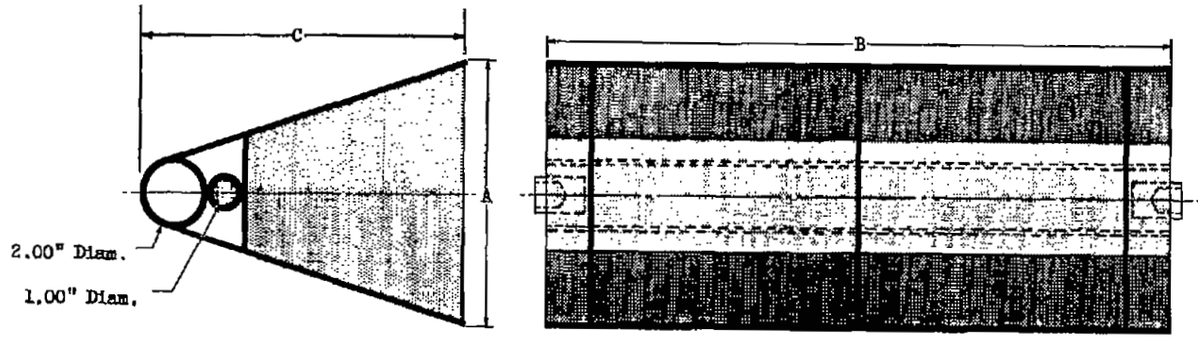

Configurations 14 and 15

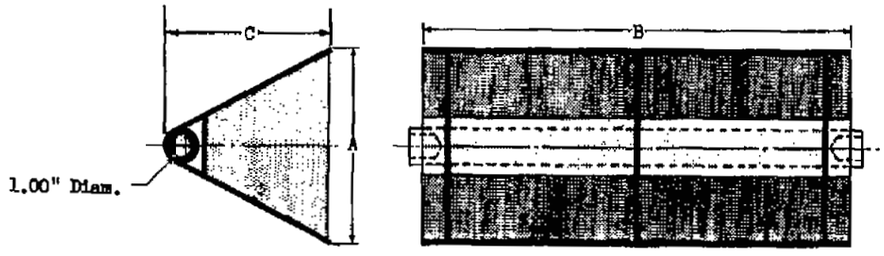

Configuration	Duct diameter, in.	A	B	C
14	20.00	7.50	19.00	6.20
15	20.00	9.00	19.00	5.75
16	14.00	4.03	15.00	3.40
17	14.00	5.50	15.00	2.90
18	8.00	2.28	7.50	2.50
19	8.00	3.80	7.50	3.10
20	8.00	Collapsed	7.50	

Configurations 16 to 20 CD-3593

(f) Diametrical flame-holder configurations used in 20-, 14-, and 8-inch ducts.

Figure 3. - Continued. Flame holders used for investigations in 28-inch duct and 32-inch afterburner. (Linear dimensions in inches).

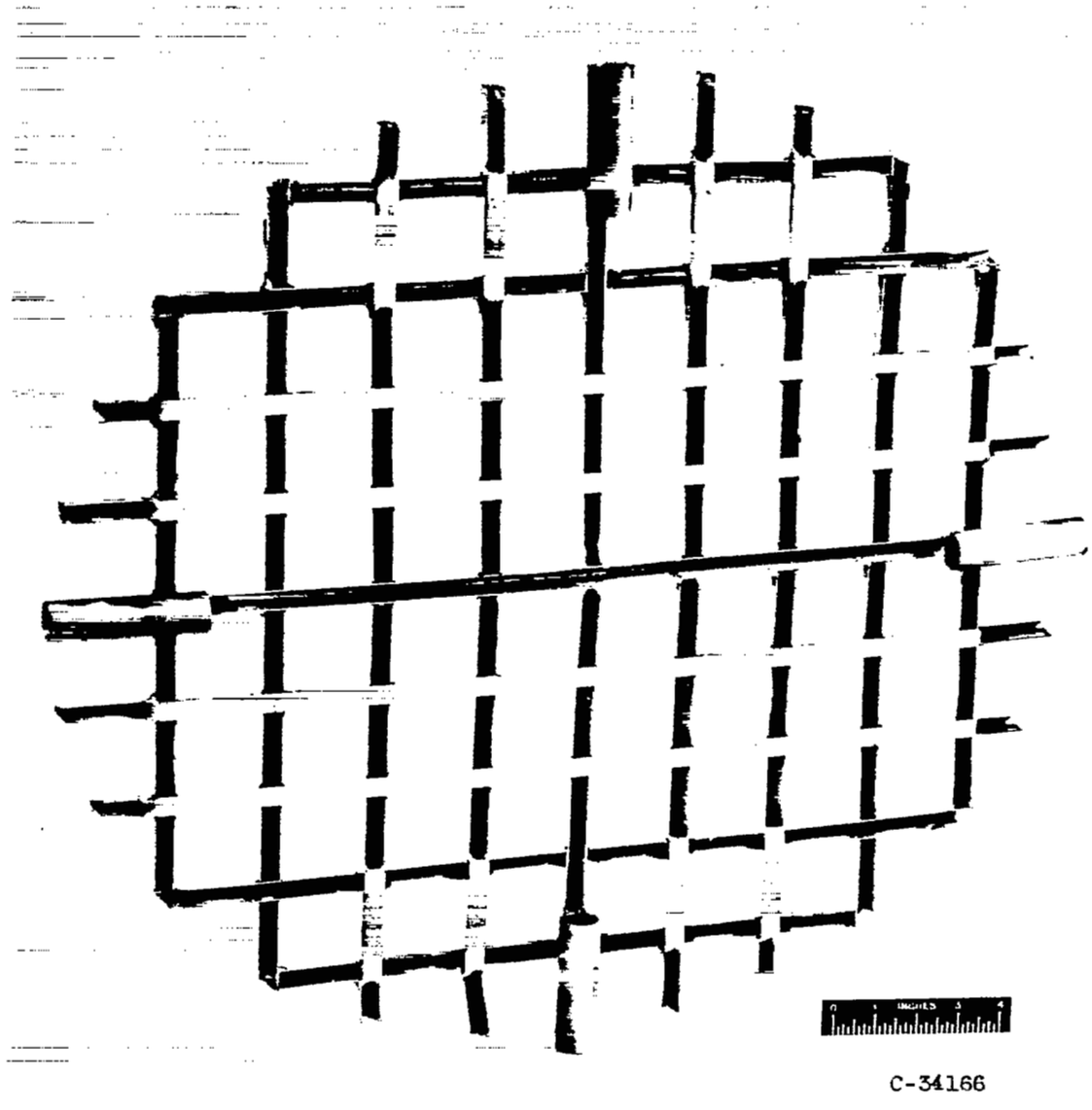

C-34166

Configuration 21

(g) Grid-type flame holder used in 26-inch duct.

Figure 3. - Continued. Flame holders used for investigations in 26-inch duct and 32-inch afterburner. (Linear dimensions in inches).

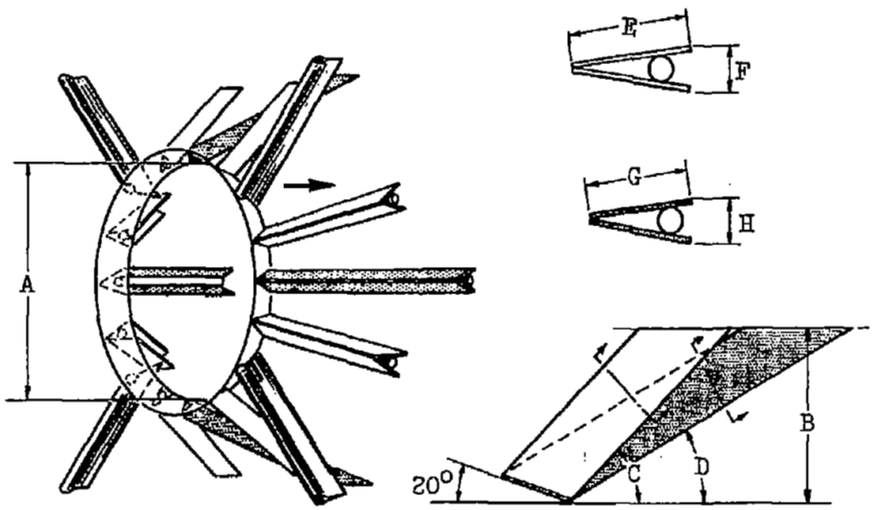

CD-3407

Configuration	A	B	Swept gutter 1				Swept gutter 2			
			C	E	F	Elements	D	G	H	Elements
22	16.00	5.80	45°	2.10	0.75	8	30°	1.80	0.75	4
23	12.00	7.87	60°	1.31	.75	8	45°	1.31	.75	8

(h) Radial-swept flame holders used in 32-inch-diameter afterburner.

Figure 3. - Concluded. Flame holders used for investigations in 26-inch duct and 32-inch afterburner. (Linear dimensions in inches).

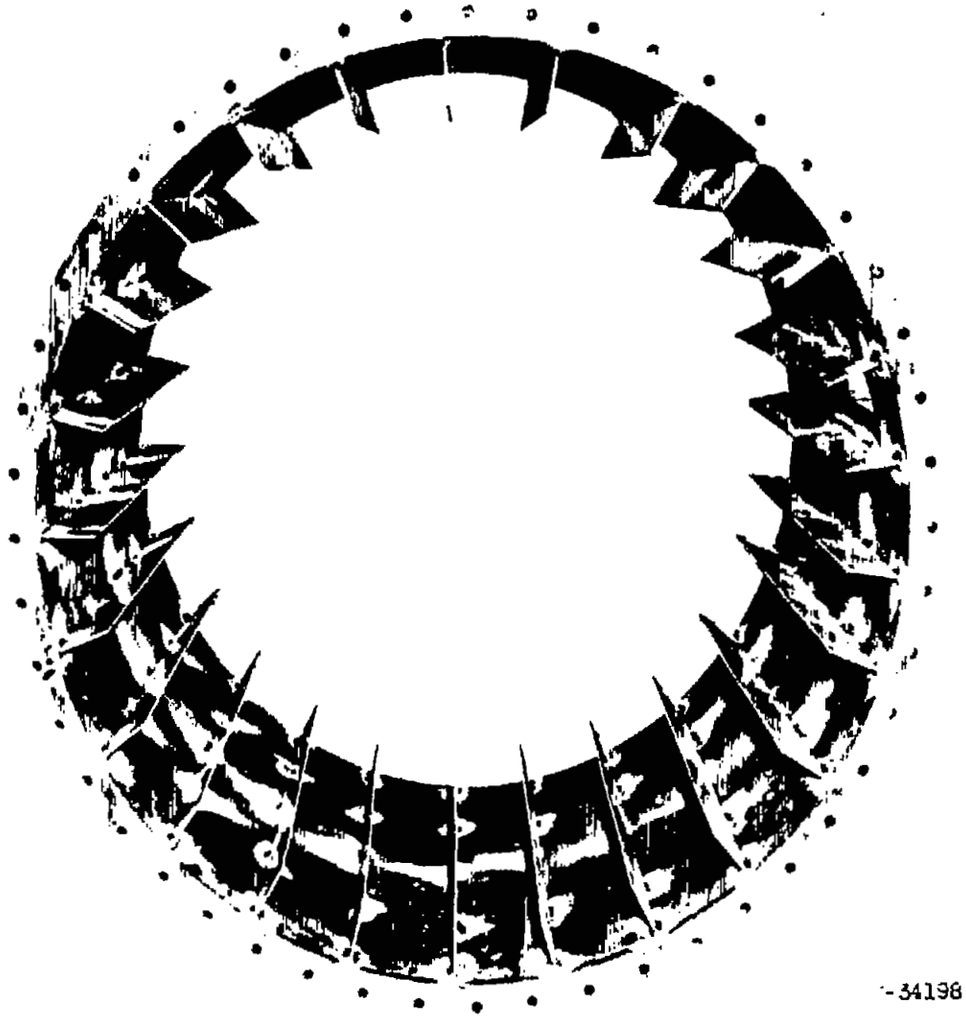

-34198

(a) Longitudinal fins installed in 32-inch-diameter short afterburner.

Figure 4. - Finned afterburner.

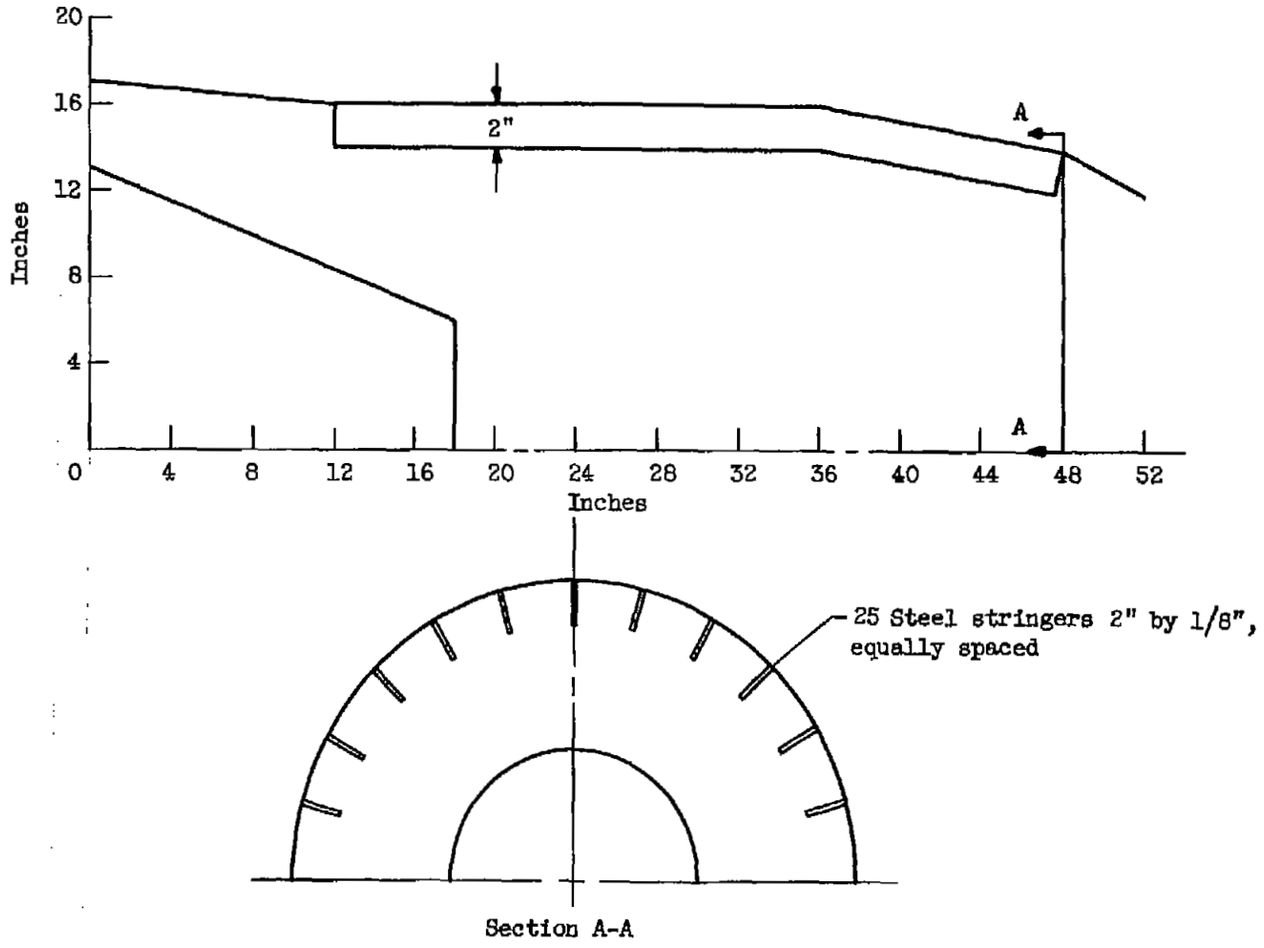

(b) Sketch of longitudinal fins installed in 32-inch-diameter short afterburner.

Figure 4. - Concluded. Finned afterburner.

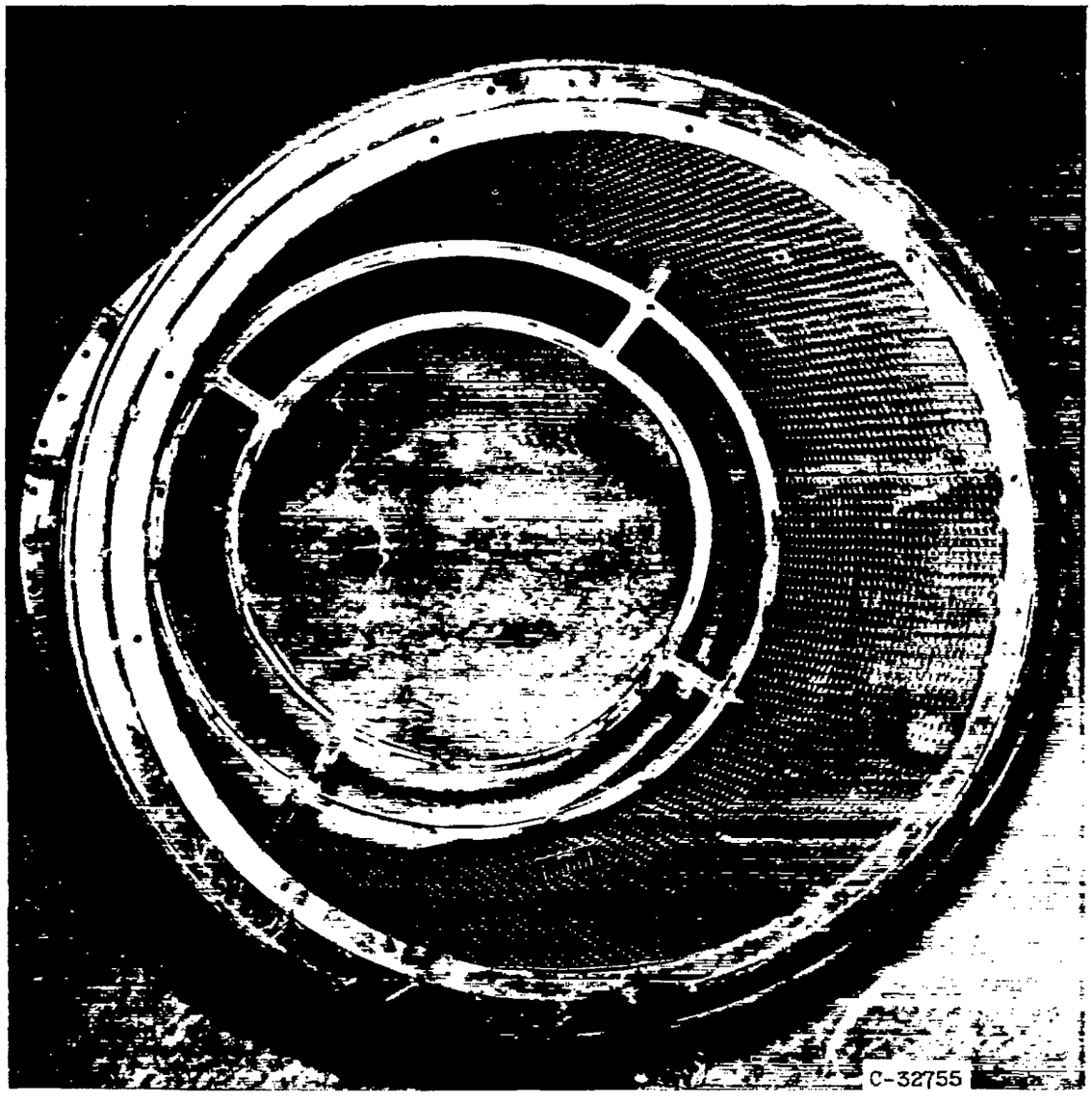

(a) Perforated acoustic liner and 3/4-inch double-ring flame holder.

Figure 5. - Perforated acoustic liner used in 32-inch-diameter short afterburner.

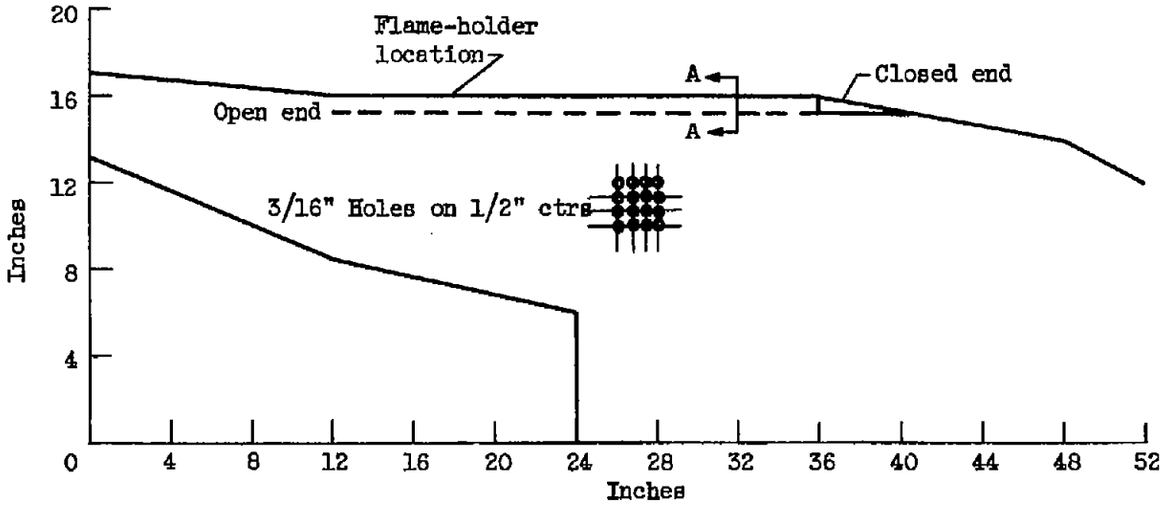

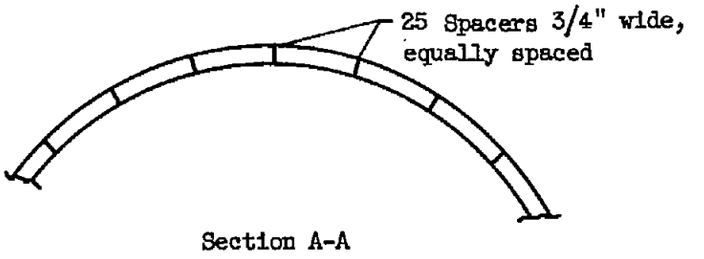

Section A-A

(b) Sketch of perforated acoustic liner.

Figure 5. - Concluded. Perforated acoustic liner used in 32-inch-diameter short afterburner.

3146

CH-5 back

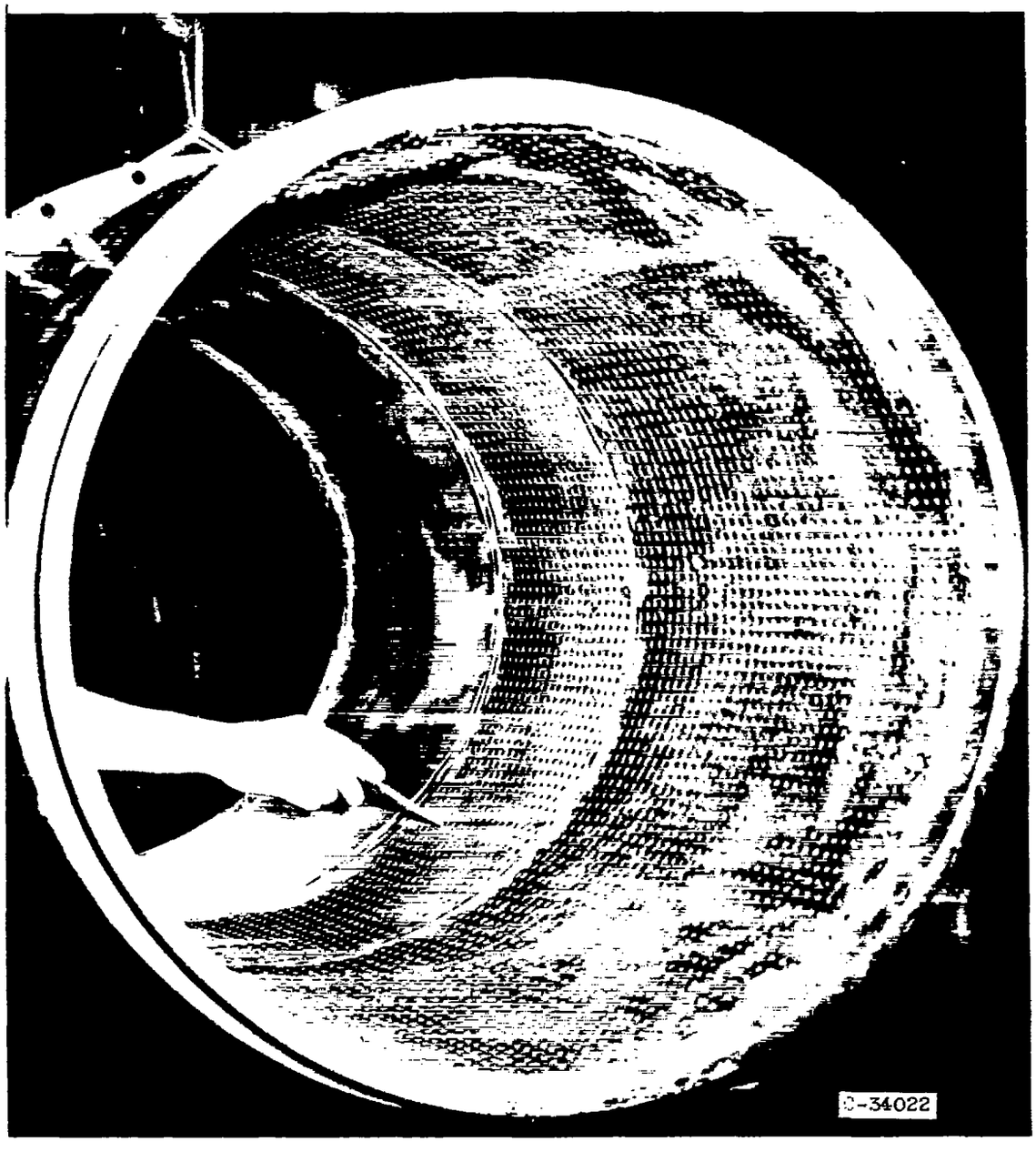

(a) 10- and 19-Inch acoustic-liner sections installed in 26-inch-diameter duct.

Figure 6. - Acoustic liner used in 26-inch-diameter duct.

[redacted]

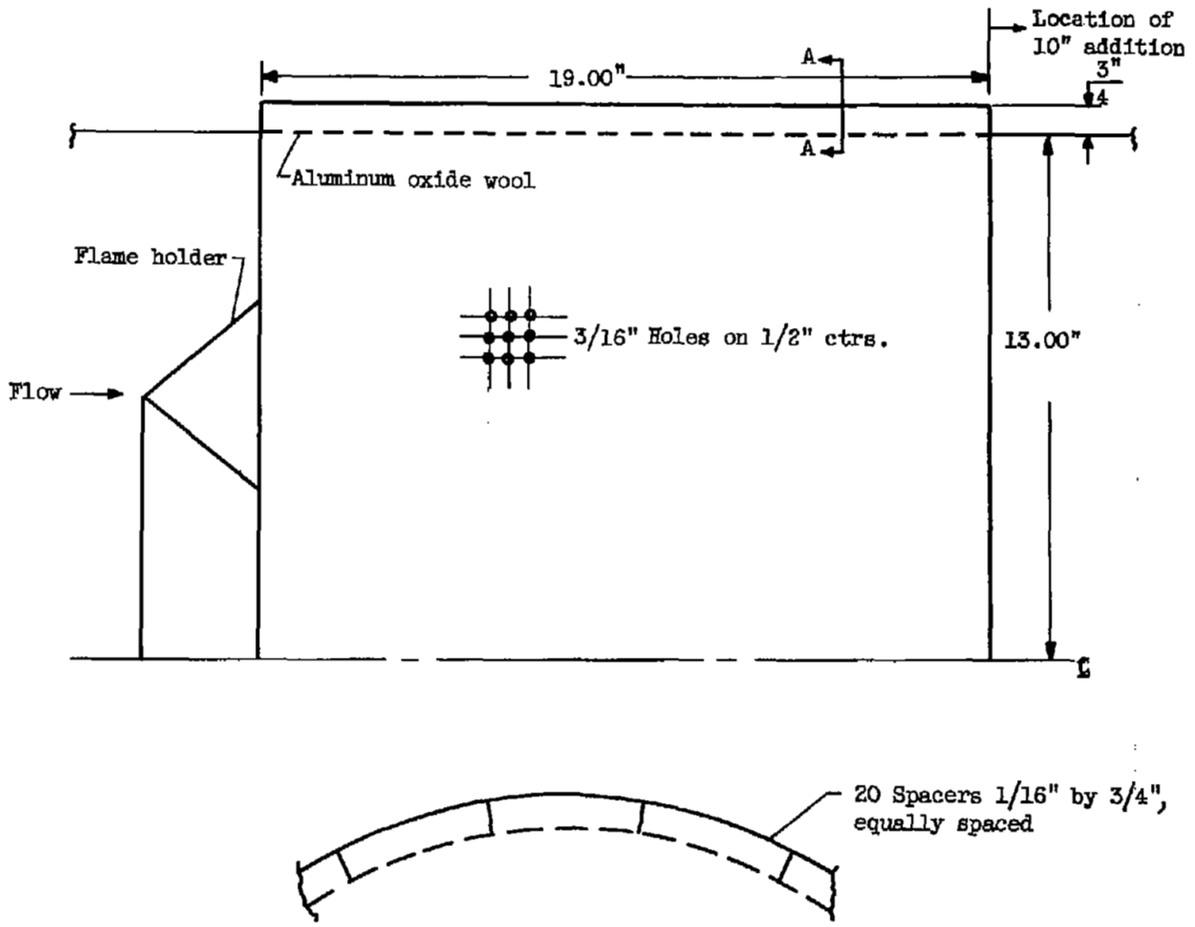

Section A-A

(b) Sketch of perforated acoustic liner.

Figure 6. - Concluded. Acoustic liner used in 26-inch-diameter duct.

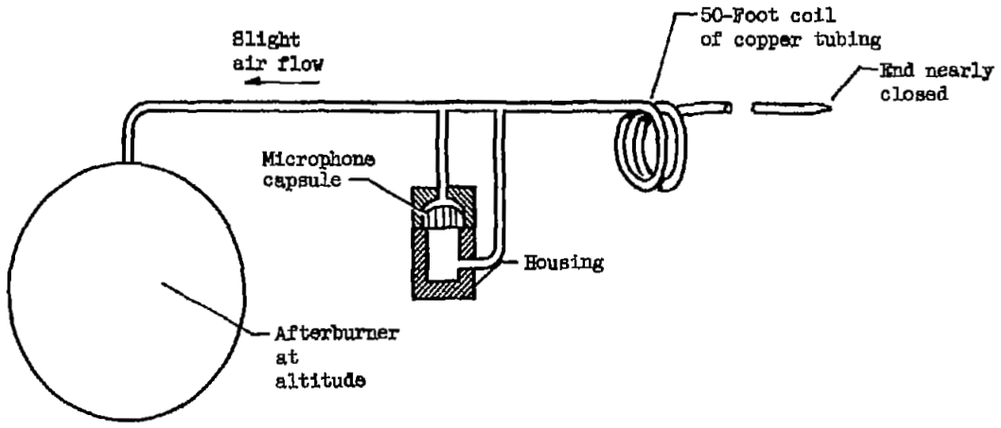

(a) Microphone-type pressure pickup.

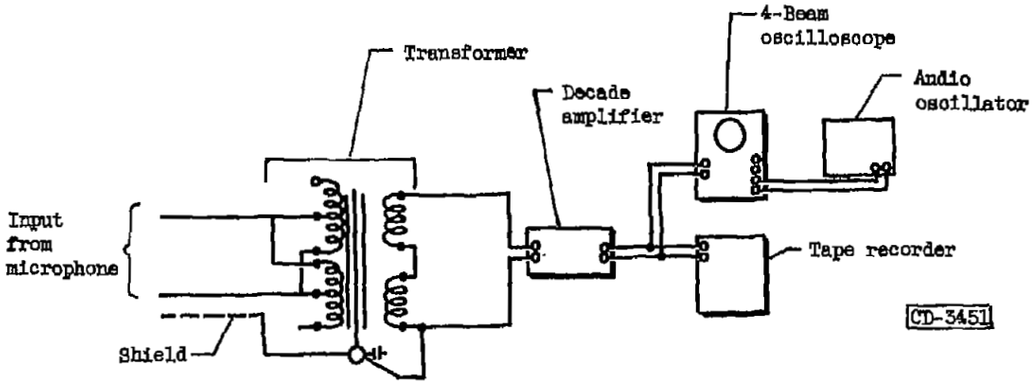

(b) Signal analyzing system.

Figure 7. - Schematic diagrams of microphone-type pressure pickup and signal analyzing system.

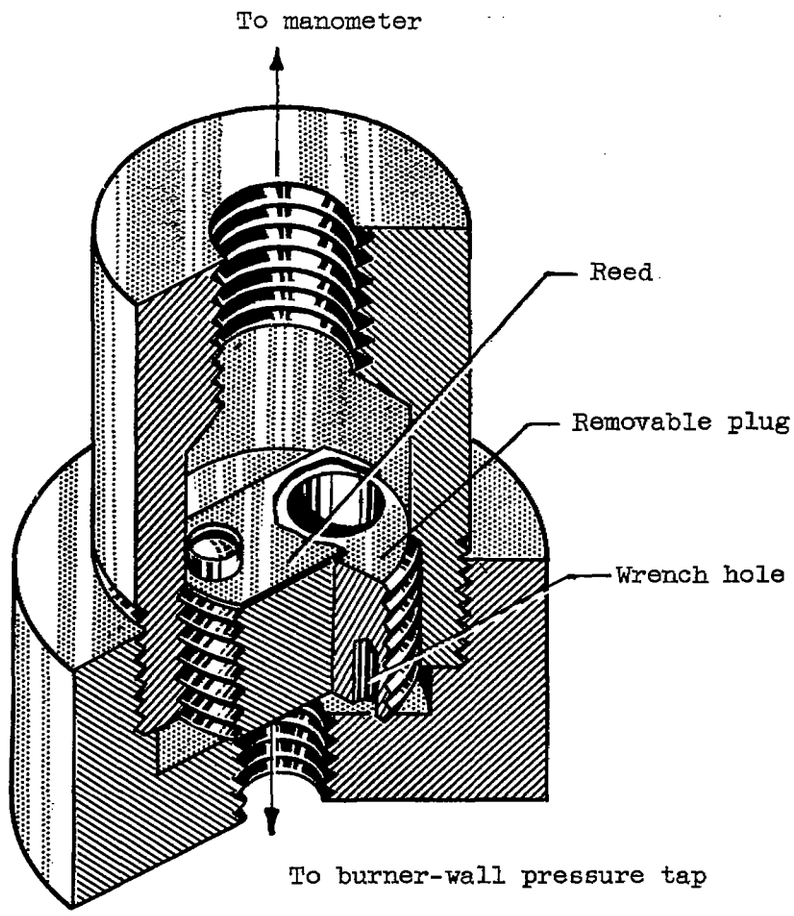

Figure 8. - Sketch of reed valve.

[redacted]

3146

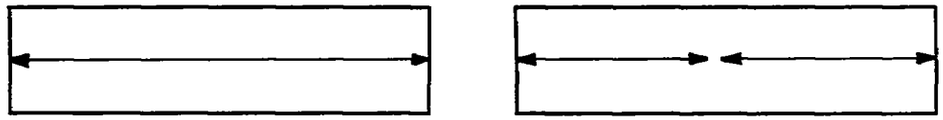

First mode Second mode

(a) Longitudinal oscillations (closed end).

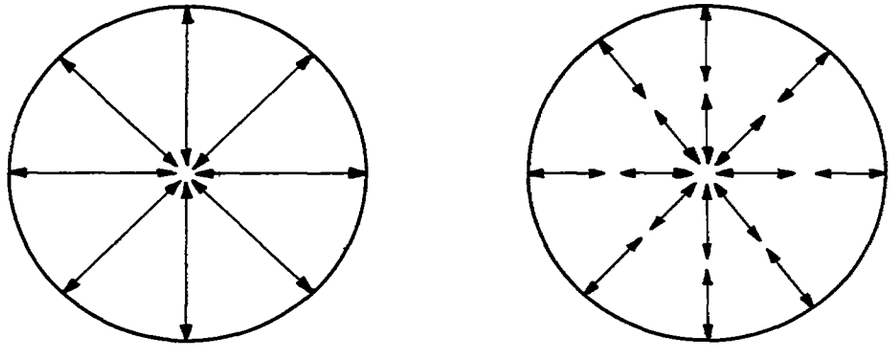

First mode Second mode

(b) Radial oscillations.

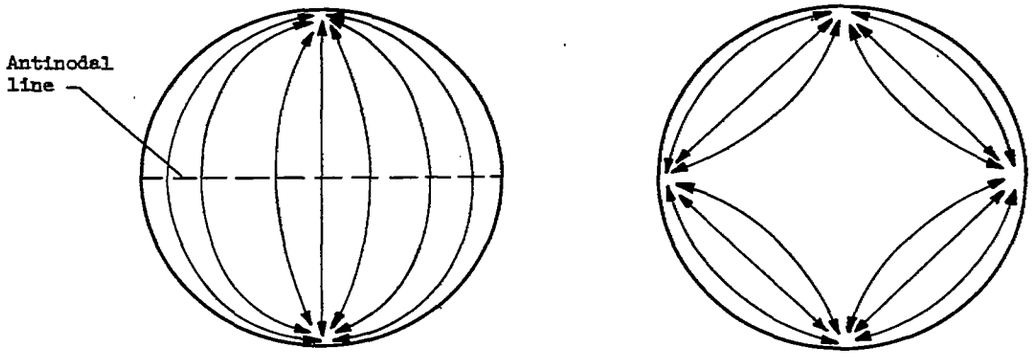

First mode Second mode

(c) Transverse oscillations.

Figure 9. - Particle paths for first and second modes of three types of acoustical resonance. Arrowheads indicate nodes.

[redacted]

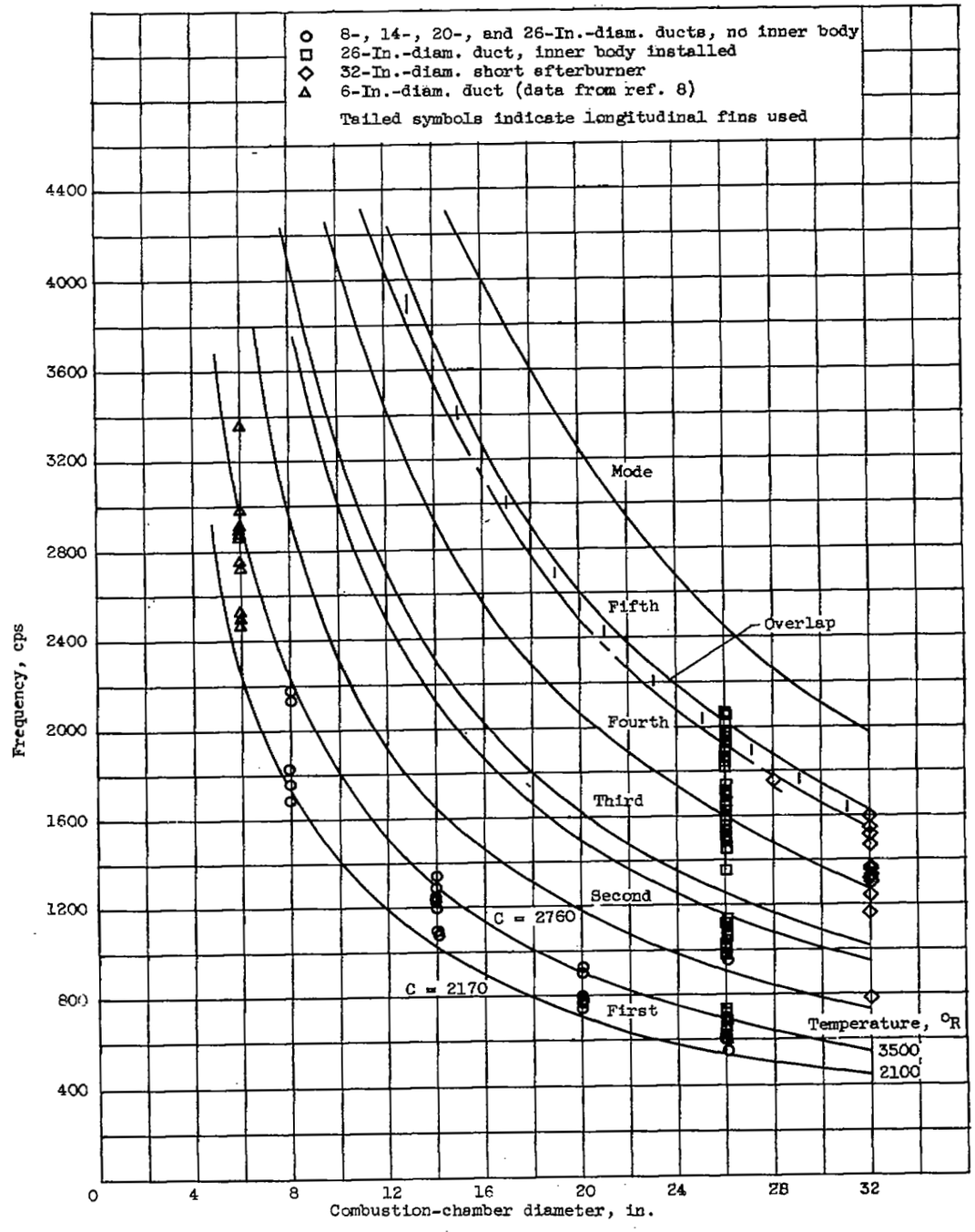

Figure 10. - Variation of frequency with burner diameter for first five transverse modes of oscillation. Average static temperatures of 2100° and 3500° R and combustion-chamber-inlet Mach number of 0.333 assumed. (C is in ft/sec.)

[redacted]

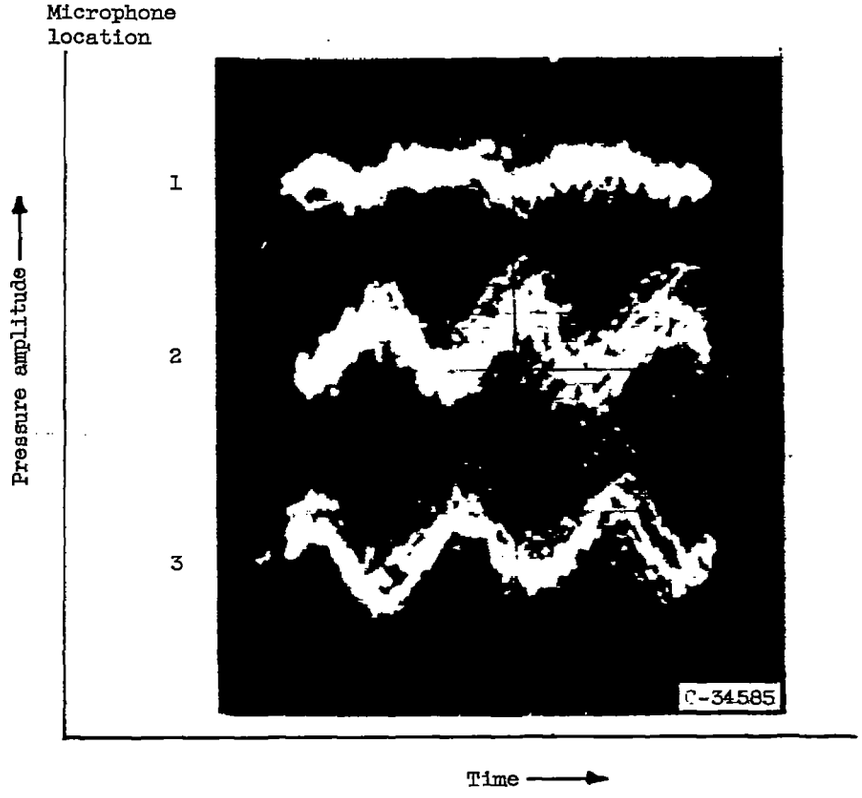

(a) Oscilliscope traces obtained with 5-inch-wide diametrical V-gutter flame holder. Microphone taps, 4.2 inches downstream of flame holder; screech frequency, 560 cycles per second.

Figure 11. - Phase relations of pressure oscillations in 26-inch-diameter duct.

[redacted]

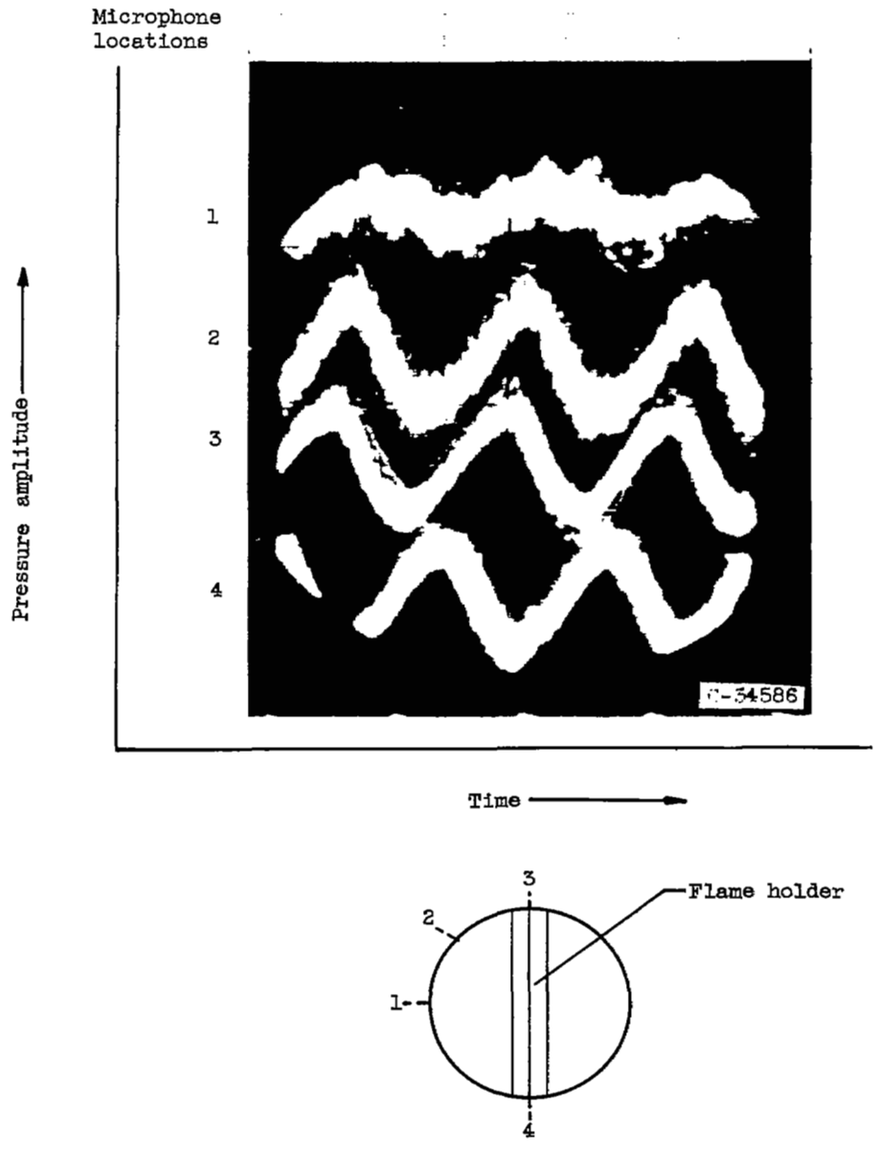

(b) Oscilliscope traces obtained with 7-inch-wide diametrical V-gutter flame holder. Microphone taps, 1.0 inch downstream of flame holder; screech frequency, 635 cycles per second.

Figure 11. - Concluded. Phase relations of pressure oscillations in 26-inch-diameter duct.

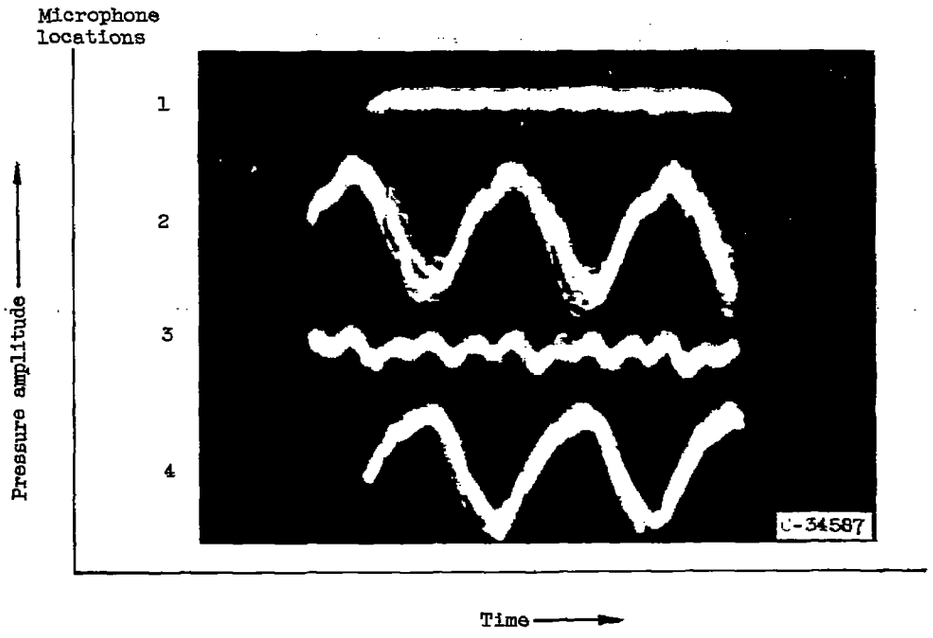

Oscilliscope traces

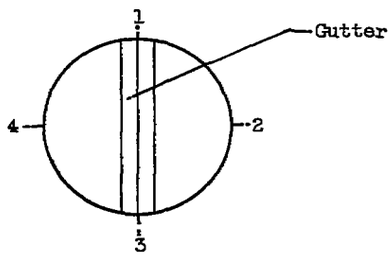

Microphone locations as seen when looking downstream

(a)

Figure 12. - Phase relations of pressure oscillations in 26-inch-diameter duct with 8-inch-wide diametrical V-gutter flame holder. Microphone taps, 1.0 inch downstream of flame holder; screech frequency, 650 cycles per second.

[redacted]

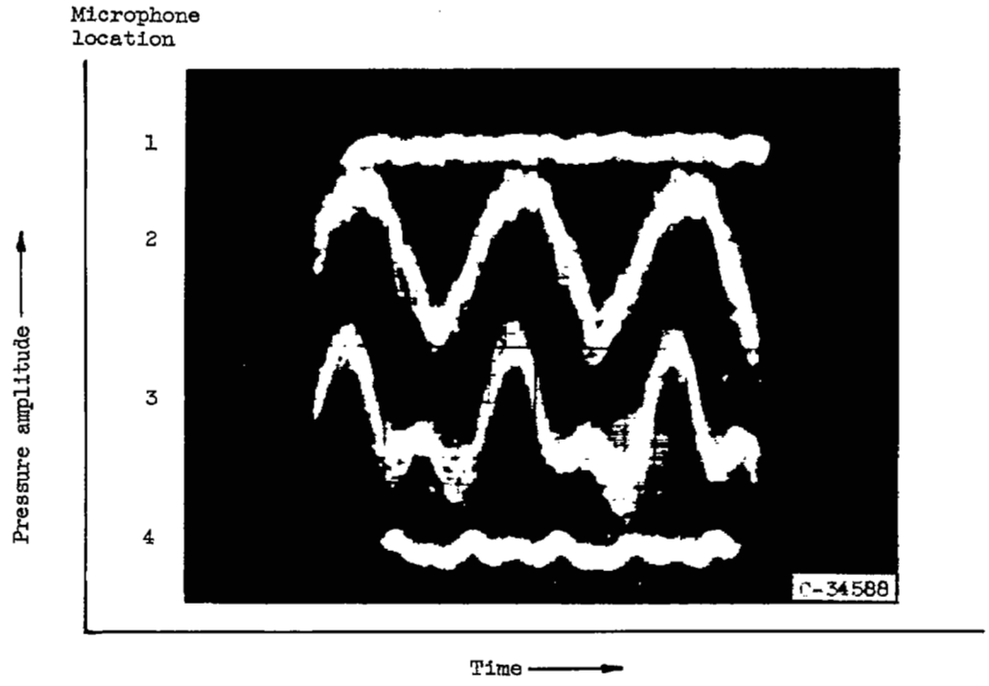

Oscilliscope traces

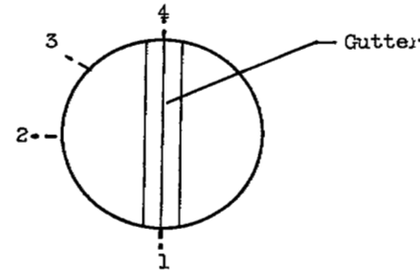

Microphone locations as seen when looking downstream

(b)

Figure 12. - Concluded. Phase relations of pressure oscillations in 26-inch-diameter duct with 8-inch-wide diametrical V-gutter flame holder. Microphone taps, 1.0 inch downstream of flame holder; screech frequency, 650 cycles per second.

[redacted]

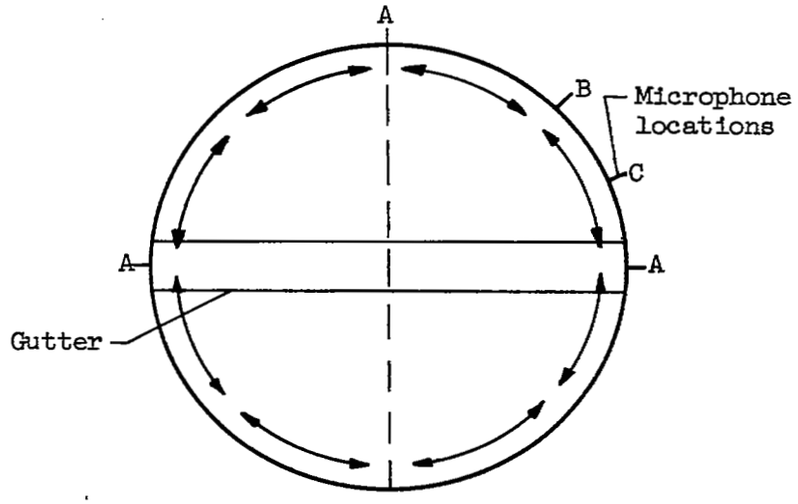

Figure 13. - Fourth transverse mode of oscillation with diametrical V-gutter installed at trailing end of inner body. Screech frequency, 1740 cycles per second; duct diameter, 26 inches.

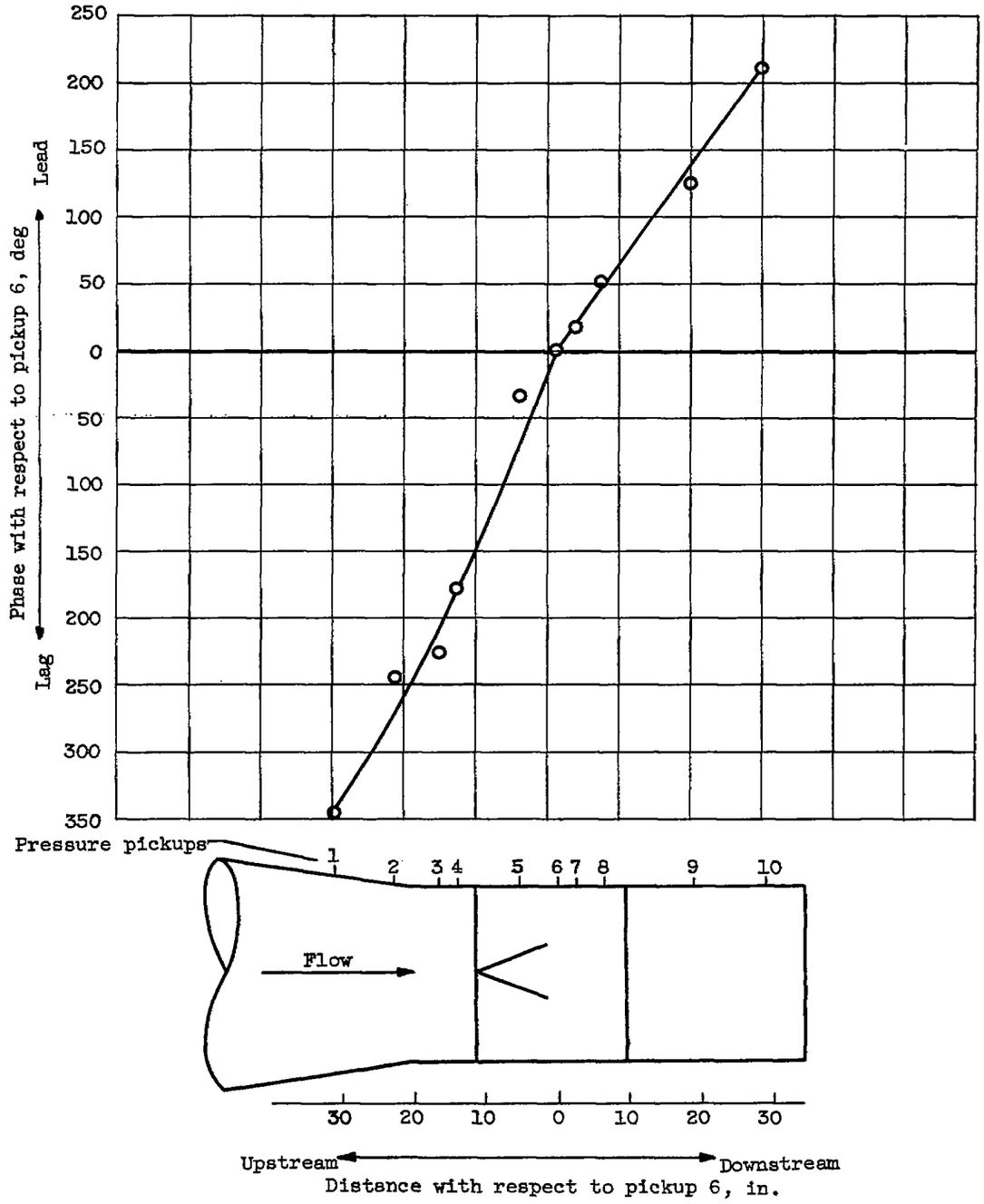

Figure 14. - Phase relations along wall of 26-inch-diameter duct. Pressure pickups located in plane perpendicularly bisecting the 8-inch-wide diametrical flameholder. Screech frequency, 650 cycles per second; over-all fuel-air ratio, 0.0622.

[redacted]

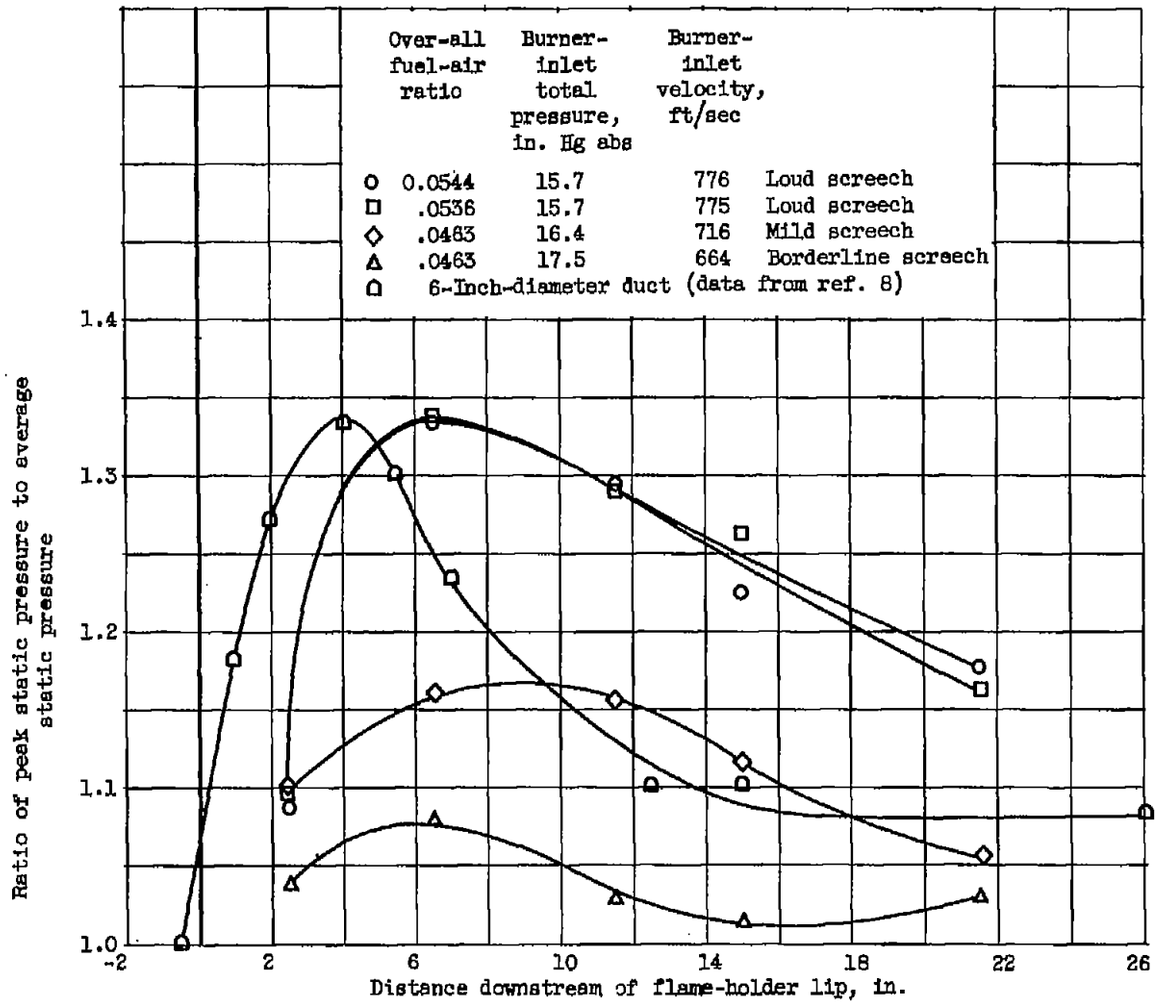

Figure 15. - Variation of ratio of peak static pressure (Reed valve) to average static pressure with distance downstream of flame holder in 26-inch-diameter duct. Air flow, 22.6 pounds per second.

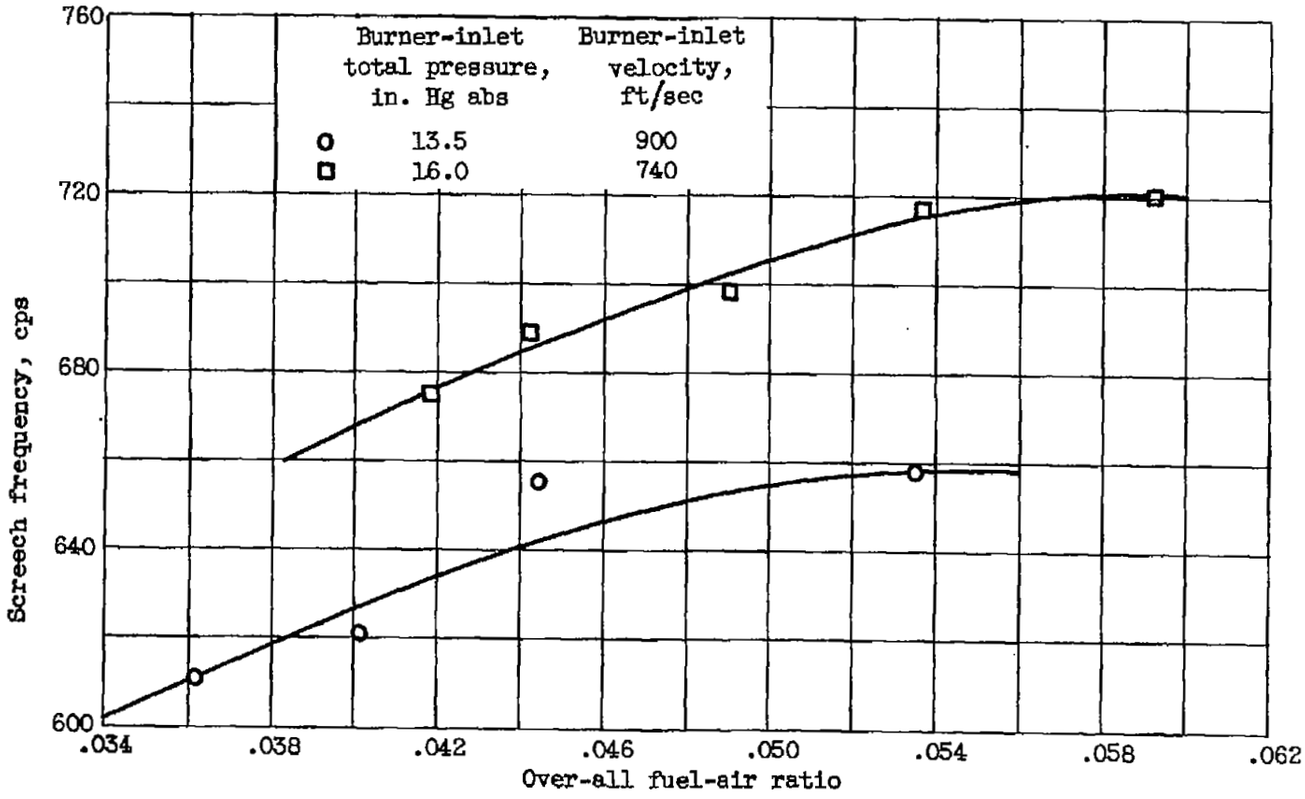

Figure 16. - Variation of frequency with fuel-air ratio at two burner-inlet total pressures in 26-inch-diameter duct with single-ring V-gutter flame holder 2.5 inches wide. Air flow, 22.6 pounds per second.

3146

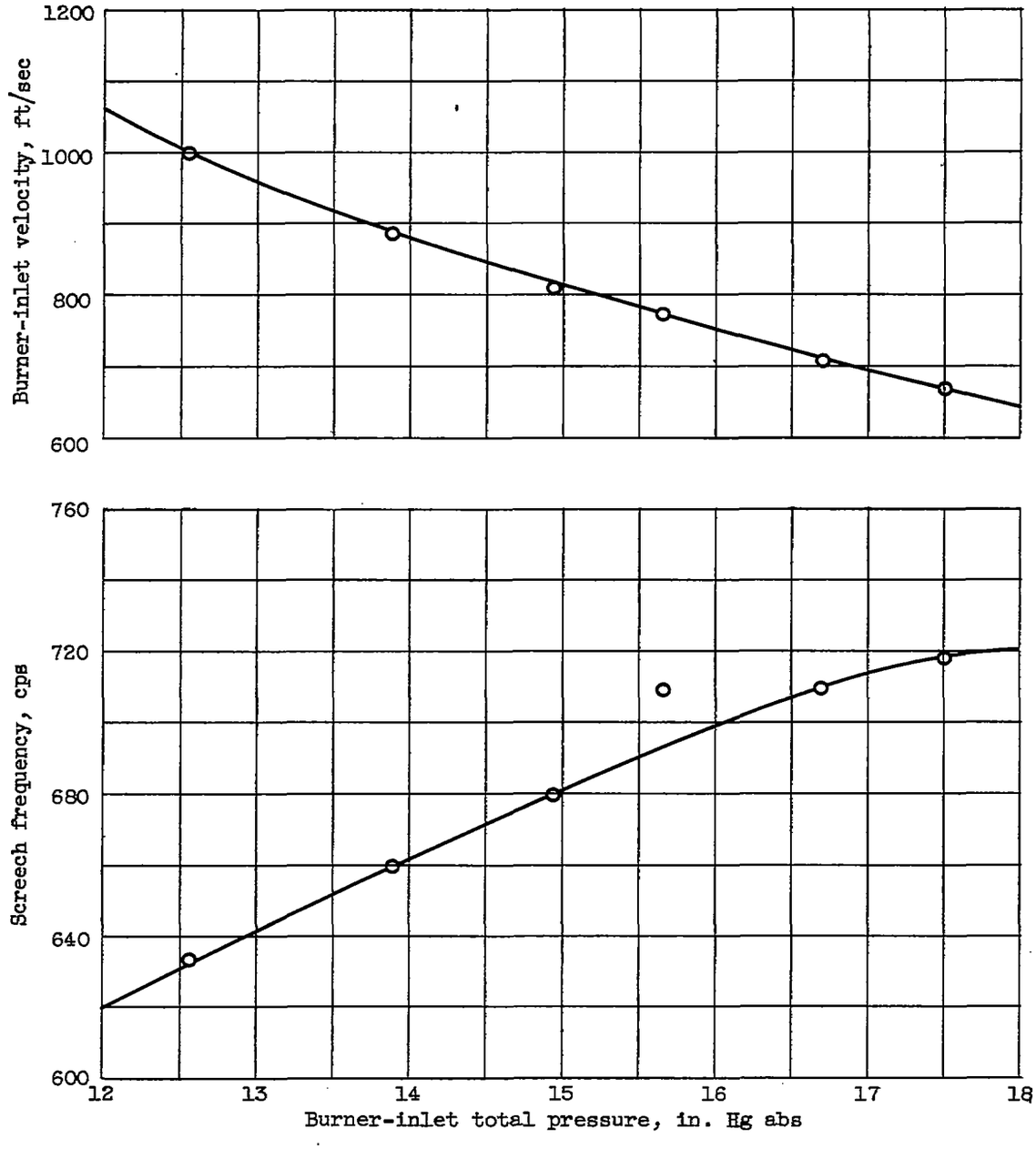

Figure 17. - Variation of screech frequency with burner-inlet velocity and burner-inlet total pressure in 26-inch-diameter duct with single-ring V-gutter flame holder 2.5 inches wide. Air flow, 22.6 pounds per second; fuel-air ratio, 0.0536.

[redacted]

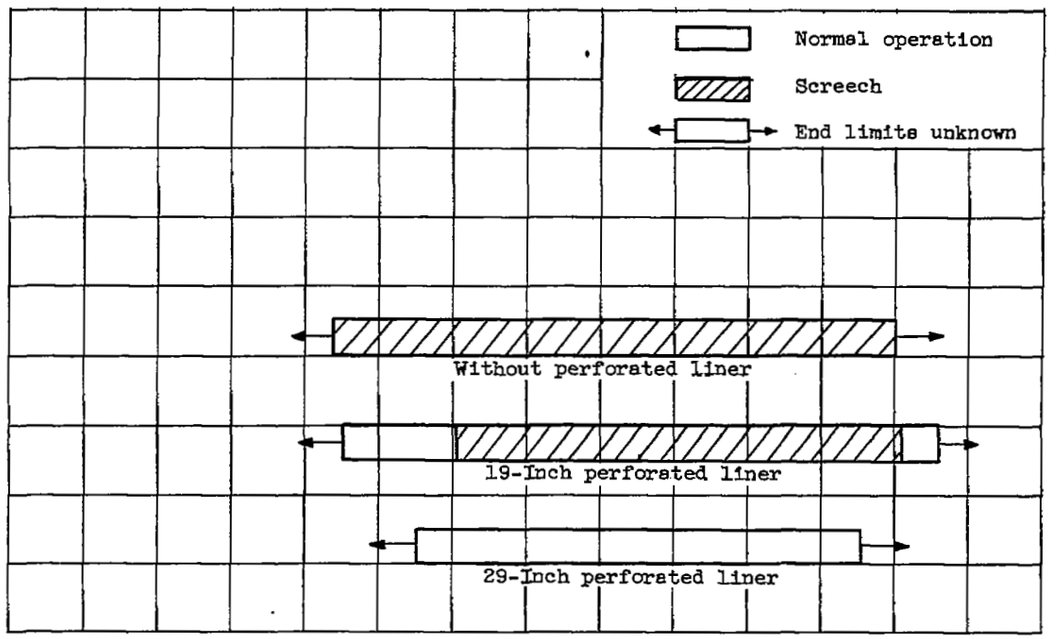

(a) Afterburner-inlet total pressure, 1750 pounds per square foot.

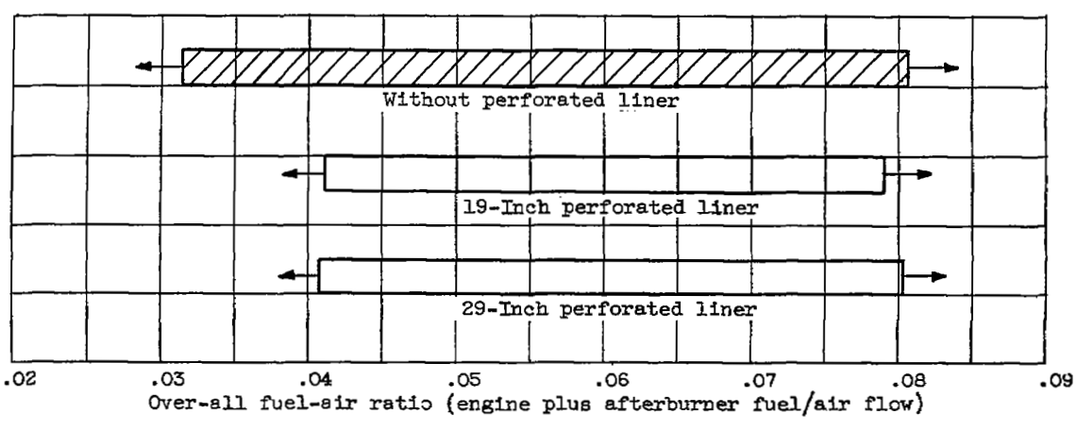

(b) Afterburner-inlet total pressure, 1400 pounds per square foot.

Figure 18. - Effect of perforated acoustic liner on screech limits. 26-Inch-diameter duct; 4.59-inch-wide single-ring flame holder.

NACA-Langley - 3-22-54 - 325